Article:
Hollaway, MJ, Arnold, SR orcid.org/0000-0002-4881-5685, Collins, WJ et al. (2 more authors) (2017) Sensitivity of mid-19th century tropospheric ozone to atmospheric chemistry-vegetation interactions. Journal of Geophysical Research: Atmospheres, 122 (4). pp. 2452-2473. ISSN 2169-897X

https://doi.org/10.1002/2016JD025462

Sensitivity of mid-19th century tropospheric ozone to atmospheric chemistry-vegetation interactions

M. J. Hollaway[1,2], S. R. Arnold[1], W. J. Collins[3,4], G. Folberth[3], and A. Rap[1]

S.R. Arnold, S.Arnold@leeds.ac.uk

[1]Institute for Climate and Atmospheric Science, School of Earth and Environment, University of Leeds, Leeds, LS2 9JT, UK

[2]now at: Lancaster Environment Centre, Lancaster University, Lancaster, LA1 4YQ UK

[3]Hadley Centre, Met Office, Fitzroy Road, Exeter, EX1 3PB, UK

[4]now at: Department of Meteorology, University Reading, Reading, UK

This article has been accepted for publication and undergone full peer review but has not been through the copyediting, typesetting, pagination and proofreading process, which may lead to differences between this version and the Version of Record. Please cite this article as doi: 10.1002/2016JD025462

Abstract. We use an Earth-System model (HadGEM2-ES) to investigate the sensitivity of mid-19th century tropospheric ozone to vegetation distribution and atmospheric chemistry-vegetation interaction processes. We conduct model experiments to isolate the response of mid-19th century tropospheric ozone to vegetation cover changes between the 1860s and present-day and to CO_2 induced changes in isoprene emissions and dry deposition over the same period. Changes in vegetation distribution and CO_2 suppression of isoprene emissions between mid-19th century and present-day, lead to decreases in global isoprene emissions of 19% and 21% respectively. This results in increases in surface ozone over the continents of up to 2 ppbv and of 2-6 ppbv in the tropical upper troposphere. The effects of CO_2 increases on suppression of isoprene emissions and suppression of dry deposition to vegetation are small compared with the effects of vegetation cover change. Assuming present-day climate in addition to present-day vegetation cover and atmospheric CO_2 concentrations, leads to increases in surface ozone concentrations of up to 5 ppbv over the entire northern hemisphere (NH), and of up to 8 ppbv in the NH free troposphere, compared with a mid-19th century simulation. Ozone changes are dominated by: 1) the role of isoprene as an ozone sink in the low NO_x mid-19th century atmosphere, and 2) the redistribution of NO_x to remote regions and the free troposphere via PAN (peroxyacetyl nitrate) formed from isoprene oxidation. We estimate a tropospheric ozone radiative forcing of 0.264 W m^{-2} and a sensitivity in ozone radiative forcing to mid-19th century to present-day vegetation cover change of -0.012 W m^{-2}.

Keypoints:

- Simulated mid-19th century ozone distribution is sensitive to assumed model vegetation distribution
- Impact of mid-19th century to present day vegetation change on tropospheric ozone dominated by change in isoprene emissions
- Ozone radiative forcing is sensitive to assumption regarding mid-19th century vegetation distribution

1. Introduction

Ozone in the troposphere is a secondary pollutant, which in addition to being a greenhouse gas, is harmful to human health, increasing mortality [*Anenberg et al.*, 2010], and is damaging to ecosystems, reducing global crop yields [*Van Dingenen et al.*, 2009; *Hollaway et al.*, 2012; *Avnery et al.*, 2013; *Tai et al.*, 2014] and inhibiting the land carbon sink [*Sitch et al.*, 2007; *Collins et al.*, 2010; *Lombardozzi et al.*, 2013, 2015; *Yue and Unger*, 2014]. Since the mid-19th century period, anthropogenic emissions of ozone precursors (NO_x, CO, CH_4 and volatile organic compounds (VOCs)) have led to increased tropospheric ozone, particularly over industrialised northern hemisphere (NH) regions [*Stevenson et al.*, 2013]. Model calculations estimate the radiative forcing due to this increase in tropospheric ozone to be 0.4 ± 0.2 (95 % confidence limit) W m^{-2} [*Myhre et al.*, 2013]. Uncertainty on this value partly results from uncertainty in processes controlling ozone concentrations in the mid-19th century, which define the baseline on top of which anthropogenic ozone precursor sources contribute. Such uncertainties include assumptions regarding mid-19th century emissions of ozone precursors from natural sources such as biomass burning and lightning [*Mickley et al.*, 2001], and differences between present day and mid-19th century climate, which affect meteorology and transport. Uncertainties in biogenic foliage emissions, soil NO_x emissions and the available land cover maps could also potentially contribute to the uncertainty in modelled mid-19th century ozone concentrations.

Mickley et al. [2001] showed that reducing NO_x emissions from lightning and soils and increasing the emission of biogenic hydrocarbons can produce lower ozone concentrations in the mid-19th century, compared to a baseline scenario where these pre-cursor sources

were held at present-day levels. This resulted in a much higher revised radiative forcing of 0.72–0.80 W m^{-2} compared to 0.44 W m^{-2} in the baseline case. This increased forcing range is substantially larger than the more recent estimates from *Myhre et al.* [2013] and those from the Atmospheric Chemistry and Climate Inter-comparison Project (ACCMIP) (0.29–0.53 W m^{-2}) [*Stevenson et al.*, 2013]. The most likely reason for the larger estimate of *Mickley et al.* [2001] is due todifferent assumptions in precursor emissions and the offline reduction in biogenic emissions. Uncertainties associated with the representation of inorganic bromine (Br_y) chemistry [*Parrella et al.*, 2012] and the magnitude of biomass burning in the mid-19th century period [*Wang and Jacob*, 1998; *Shindell et al.*, 2003; *Lamarque et al.*, 2005; *Rap et al.*, 2015] also lead to poor constraint on the mid-19th century ozone distribution. This is demonstrated by the findings of *Rap et al.* [2015] where the introduction of present day biomass burning emissions in the mid-19th century produced a reduction in the calculated ozone radiative forcing from 0.32 W m^{-2} to 0.23 W m^{-2}.

Additional influences on the change between mid-19th century and present day tropospheric ozone also result from changes in land cover. Emissions of BVOCs such as isoprene, are highly sensitive to vegetation type and foliage density (leaf area index) [*Niinemets et al.*, 2010a, b; *Guenther et al.*, 2006], as well as environmental controls such as light [*Monson and Fall*, 1989; *Strada and Unger*, 2016], temperature [*Guenther et al.*, 1993], atmospheric CO_2 [*Monson et al.*, 2007] and soil moisture [*Pegoraro et al.*, 2004; *Monson et al.*, 2007]. The rate of isoprene emission increases with temperature until an optimum of about 40°C [*Niinemets et al.*, 1999], however evidence suggests that this can vary between plant species and can be affected by plants becoming acclimatized to their

conditions [*Wilkinson et al.*, 2009; *Niinemets and Sun*, 2015]. Conversely, measurements have shown increased ambient CO_2 concentrations inhibit isoprene emission [*Possell et al.*, 2005; *Wilkinson et al.*, 2009], with the potential of different response patterns to short and long term changes in the atmospheric CO_2 burden [*Young et al.*, 2009; *Pacifico et al.*, 2009]. Accordingly, changes in vegetation distributions and environmental drivers between mid-19th century and present-day are expected to result in changes in the distribution and magnitude of global isoprene emissions. Changes in both the magnitude and spatial distribution of isoprene emissions can lead to enhanced ozone production or enhanced ozone loss, depending on the local NO_x burden [*Sillman*, 2000; *Ryerson et al.*, 2001; *Arneth et al.*, 2007]. A recent study attributed a substantial negative ozone radiative forcing (-0.13 W m^{-2}) to a reduction in forest tree cover since the mid-19th century, and the associated decrease in isoprene emissions [*Unger*, 2014]. Isoprene oxidation in the presence of NO_x can also result in the formation of peroxyacetylnitrate (PAN) which can act as reservoir species for NO_x enabling long-range transport of reactive nitrogen, leading to ozone production in regions remote from ozone precursor emissions [*Wang et al.*, 1998].

Furthermore, in the tropics, where large isoprene sources may coincide with sources of NO_x from biomass burning or lightning [*Guenther et al.*, 2006; *Lelieveld et al.*, 2008], the formation of PAN can coincide with areas of deep convection which can result in its rapid transportation to the free troposphere. Here, temperatures are sufficiently low for PAN to remain stable and be transported over long distances [*Moxim et al.*, 1996], and further contribute to ozone production in remote regions. This implies a strong sensitivity of the large-scale impact of isoprene on tropospheric ozone to assumptions regarding NO_x emissions.

Vegetation cover also has a significant impact on dry deposition. The dominant pathway for dry deposition loss of ozone, and its precursors, is uptake to vegetation, by direct uptake through plant stomata and deposition to the leaf cuticular surface [*Wesely*, 1989; *Smith et al.*, 2000]. Consequently, rates of dry deposition of ozone and its precursor species (including NO_x, PAN, and other reactive nitrogen species) are highly sensitive to land cover and treatments of model vegetation [*Ganzeveld and Lelieveld*, 1995; *Giannakopoulos et al.*, 1999; *ValMartin et al.*, 2014]. In addition, the ambient atmospheric CO_2 concentration can influence the rate of dry deposition due to higher CO_2 concentrations inducing stomatal closure and hence reducing the rate of trace gas exchange between the atmosphere and vegetation [*Gedney et al.*, 2006].

The effects of vegetation cover and CO_2 change on isoprene emissions and dry deposition resectively have been shown to have competing impacts on tropospheric ozone concentrations [*Wu et al.*, 2012; *Fu and Tai*, 2015]. For example, *Fu and Tai* [2015] demostrated that in the high NO_x, VOC-limited regime over many parts of central China, despite increases in isoprene emissions ozone concentrations were estimated to decrease. It was shown that eleveted summertime Leaf Area Index (LAI) enhanced dry deposition and thus dominated the small rise in ozone from enhanced isoprene. In contrast, in the NO_x limited parts of western China, reductions in isoprene emissions were shown to dominate and despite higher dry deposition over these regions, ozone levels were shown to increase [*Fu and Tai*, 2015]. Furthermore, it has been shown that the type of vegetation (E.g. Forest versus Cropland) and anthropogenic emissions changes can also play a strong role in determining whether the isoprene or dry deposition effect dominantes the response of

modelled surface ozone to a change in vegetation cover [*Wu et al.*, 2012; *Fu and Tai*, 2015].

In this study, we use a coupled global Earth System (ES) model to investigate how changes in interactions between vegetation and atmospheric composition between 1865 and near present day (here defined as the year 2000) impact tropospheric ozone abundances and radiative forcing. We use a coupled land surface-atmospheric chemistry-climate configuration of the HadGEM2-ES model, which includes photosynthesis-driven biogenic VOC emissions from vegetation, and explicitly links vegetation stomatal conductance to reactive trace-gas dry deposition. We separately assess the impacts of the 1865 to present day changes in land surface cover, climate and atmospheric CO_2 on the dry deposition of ozone and its precursors, and biogenic isoprene emissions (fast responses due to impacts on photosynthesis rather than long term responses due to changes in vegetation distribution), and the resultant effects on the simulated mid-19th century tropospheric ozone distribution. The effect of these land cover-driven changes on the estimated mid-19th century to present day tropospheric ozone radiative forcing is also quantified. The HadGEM2-ES Earth-System model and model scenarios are described in Sect. 2. Section 3 presents the impacts of changing model atmospheric chemistry-vegetation interactions on atmospheric composition, focussing on tropospheric ozone and its precursor species. Section 4 presents the impact of these land cover-driven changes on the tropospheric ozone burden in the mid-19th century and the associated impact on the radiative forcing. Finally, conclusions are presented in Sect. 5.

2. Model description and scenarios

2.1. The HadGEM2-ES Earth System model

We use the global 3-D HadGEM2-ES model [*Collins et al.*, 2011] to simulate atmospheric chemistry, climate and land surface for the mid-19th century period and for present day. The model has a horizontal resolution of 1.9° by 1.3°, with 38 hybrid height levels which extend from the surface up to an altitude of approximately 39 km. The model is run in free-running atmosphere mode, with prescribed sea surface temperatures, and radiation forced by offline fields of greenhouse gas and aerosol concentrations. An explicit simulation of the land surface is included from the MOSES II scheme [*Essery et al.*, 2003], including vegetation photosynthesis and stomatal conductance, driven by model climate and ambient CO_2, which directly affects dry deposition and biogenic emissions. The effects of simulated atmospheric concentrations of ozone and aerosol on the climate via interactions with the model radiation scheme or carbon cycle are not included.

The extended chemistry version of the UK Community Chemistry and Aerosol (UKCA) scheme is used to simulate atmospheric composition, featuring approximately 200 chemical reactions and accounting for 83 species. The scheme includes tropospheric CH_4-NO_x-CO-O_3 chemistry [*O'Connor et al.*, 2014] with the addition of simplified isoprene reactions [*Folberth et al.*, 2006; *Pacifico et al.*, 2015] based on the Mainz Isoprene Mechanism (MIM) [*Poschl et al.*, 2000]. In this study an updated version of the MIM was utilised where the rate coefficients of nitrogen containing organic compounds were improved (Jenkin, personal communication) based on the latest release of the Leeds master chemical mechanism (MCM: http://mcm.leeds.ac.uk/MCM/). This version of the MIM was recently used by *Pacifico et al.* [2015] to simulate the impacts of biomass burning induced ozone damage on vegetation in the Amazon rainforest and was shown to perform well compared to observations over the region. This demonstrates that the updated MIM performs well

under low NO_x-high isoprene conditions and is suitable to model the impacts of changing atmospheric chemistry-vegetation interactions in the mid 19th century.

For the treatment of dry deposition of gas phase species and aerosols, a big leaf model approach is used as described by *Sanderson et al.* [2006], which uses stomatal conductance and leaf area index (LAI) from the model vegetation scheme. Biogenic emissions of isoprene, a lumped monoterpene species, acetone and methanol are calculated online using the interactive emissions scheme. The isoprene emissions scheme, as described by *Pacifico et al.* [2011] calculates the rate of isoprene synthase and emission based upon vegetation type and the rate of photosynthesis and dark respiration from the MOSES simulation. The CO_2 inhibition effect on isoprene emissions is accounted for using an empirical based relationship derived from *Arneth et al.* [2007], which is dependent on the internal CO_2 concentration of the leaf and also includes the short-term response of emissions to drought stress [*Arneth et al.*, 2007]. Finally, emissions of NO_x from lightning are determined interactively according to *Price and Rind* [1993]. Anthropogenic surface emissions are taken from the historical (1850 to 2000) gridded emissions dataset used for the Climate Model Intercomparison Program #5 (CMIP5) simulations [*Lamarque et al.*, 2010].

2.2. Prescribed model vegetation

For all of the simulations, model land cover is prescribed from a dataset representative of historical changes in land use for the period 1750–2010, as produced for CMIP5 [*Hurtt et al.*, 2011]. This data is derived from the present-day climatology IGBP dataset [*Loveland et al.*, 2000] and reconstructions of anthropogenic land-use from the HYDE3 dataset [*Klein Goldewijk et al.*, 2010]. Each model gridbox area is partitioned into frac-

tional coverage of 9 land surface types. These represent 5 plant functional types (PFTs): broadleaf tree, needleleaf tree, C3 Grasses, C4 Grasses and shrubs, plus 4 other land categories: urban, water, desert/bare ground, land ice/glacier. For each model simulation the land cover distribution is fixed, and set to update leaf phenology on a daily basis which determines the evolution of model LAI.

2.3. Model Scenarios

For the mid-19th century control run (PI_CTRL) the model was driven using sea surface temperatures (SSTs) and sea-ice fields which were representative of the period 1860-1870 and varied on a monthly basis. Anthropogenic surface emissions for the 1860s and greenhouse gas concentrations were held fixed at 1860s concentrations (286 ppmv for CO_2, 0.8 ppmv for CH_4 and 276 ppbv for N_2O [*Jones et al.*, 2011]). The model was spun-up for a period of nine months and then run for 10 years with the analysis performed on climatological averages over the last 8 years of the simulation. This relatively short spin-up period is possible as we prescribe the slow, long-term responses of the vegetation to changes in CO_2 (i.e. vegetation dynamics), rather than simulate them interactively. This is done through prescribed land cover from the HYDE3 and IGBP datasets which have explicitly accounted for both natural and antrhopogenic influences on the global vegetation distribution since the 1860s. Furthermore, by using fixed SSTs and greenhouse gas concentrations, and disabling feedbacks from changes in atmospheric ozone and aerosol to the radiation scheme, these climatological averages are sufficient to produce stable, robust tropospheric distributions of ozone and associated trace gases consistent with the driving climate and land cover conditions.

An additional set of 2 simulations were run in order to test separately the sensitivity of the modelled mid-19th century tropospheric ozone distribution to changes in land cover and climate. As with the PI_CTRL run, both of these scenarios were run for 10 years with the analysis performed on climatological averages of the last 8 years of the simulation. For the first simulation (VEG_2000), the prescribed model vegetation distribution was changed to be representative of the year 2000. This allowed the impacts of mid-19th century to present-day vegetation changes on dry deposition and BVOC emissions to be simulated. The second simulation assessed the sensitivity of mid-19th century tropospheric ozone to both changes in vegetation processes and model climate. For this simulation (CLIM_2000) the model was set up to simulate a present-day climate with fixed greenhouse gases and vegetation representative of the year 2000 (see Table 1). SSTs and sea-ice fields were also representative of the year 2000 and are prescribed as climatological monthly means for this simulation. For the CLIM_2000 simulation, the atmospheric chemistry scheme was driven using CH_4 representative of the mid-19th century period (1860s). Anthropogenic surface emissions for the 1860s were retained. The setup of this CLIM_2000 scenario is equivalent to some previous model studies investigating mid-19th century ozone in chemical transport models using prescribed offline meteorology for present day [*Hauglustaine and Brasseur*, 2001; *Lamarque et al.*, 2005; *Mickley et al.*, 2001]. For each of these additional scenarios, the model was also run for 10 years with the analysis performed on climatological averages over the last 8 years of the simulation.

Two further simulations were run to assess the sensitivity of ozone concentrations to variations in the prescribed CO_2 mixing ratio that is specified for the model vegetation scheme (CO_{2Veg}). For these simulations, the model is modified such that CO_{2Veg} only

impacts the model vegetation scheme and therefore only affects the simulated dry deposition and isoprene emissions. The standard CO_2 greenhouse gas concentration specified for the model climate simulation, is specified separately and feeds through to the rest of the model, including the carbon cycle. Furthermore, the CO_{2Veg} can be set to affect either dry deposition or isoprene emissions in isolation or both together. As a result the change in CO_{2Veg} does not feedback to photosynthesis and therefore CO_2 fertilistation of LAI is not affected in these scenarios. For the CO2_DD simulation, a CO_{2Veg} mixing ratio of 368 ppmv (representative of the year 2000) was specified, with the effects of this higher CO_{2Veg} being limited to the dry deposition (through stomatal uptake) of atmospheric trace species only. For the CO2_DDBVOC simulation, the CO_{2Veg} mixing ratio of 368 ppmv impacts both the stomatal uptake of trace species and also the emission of BVOCs through the land model iBVOC scheme. For both of these simulations the impacts of higher CO_{2Veg} concentrations affect the chemistry only and do not feedback on the model climate through impacts on the carbon cycle and water transpiration, with the rest of the model processes forced by a standard mid-19th century concentration of 286 ppmv. The CO2_DD and CO2_DDBVOC simulations are spun up for a period of nine months and then run for 3 years with the analysis performed on the final year of each run. In order to assess the impact of changing CO_{2Veg} on ozone concentrations, we took the corresponding year from the PI_CTRL for comparison. Shorter simulations are sufficient in these cases, since the simulated changes in dry deposition and biogenic emissions only impact the simulated chemical composition of the atmosphere, which does not feed back to the model radiation scheme and dynamics. These additional scenarios are summarised in Table 1.

The main aim of this study is to highlight the sensitivity of the simulated mid-19th century tropospheric ozone distribution to the model prescribed vegetation cover and assumed atmospheric chemistry-vegetation interactions (namely the effect of CO_2 on dry deposition and isoprene emissions). Therefore in order to explicitly isolate the responses of these changes and to estimate the model response in a mid-19th century atmosphere we fix anthropogenic emissions at values representative of the 1860s. Figure 1 a,c,e shows anthropogenic NO_x emissions for 1865 where global annual emissions are estimated at $34.3\,TgNO_xyr^{-1}$. As shown in Figure 1 b,d,f show that emissions of NO_x are considerably larger in 2000, with global annual emissions a factor of 4 larger at $138.1\,TgNO_xyr^{-1}$), with the largest increases seen over the major industrialised regions of North America, Europe and SE Asia. Holding emissions fixed at 1865 levels ensures that the differences between simulations are due to atmospheric-chemistry vegetation interactions rather than changes in the NO_x regime.

Finally, a near present-day (PD_2000) scenario was simulated to evaluate 1865 to 2000 changes in the tropospheric ozone burden and resultant radiative forcing. For this simulation, the model used climatological monthly mean sea surface temperatures (SSTs) and sea-ice fields representative of the 2000s. Anthropogenic surface emissions were prescribed from the CMIP5 and were set at levels representative of 2000s and greenhouse gases were held fixed at 2000s concentrations (368 ppmv for CO_2, 1.7 ppmv for CH_4 and 330 ppbv for N_2O [*Jones et al.*, 2011]). A summary of the PD_2000 is shown in Table 1.

2.4. 1865 to 2000 Land Cover Changes

Table 2 shows changes in global and regional distributions of the five vegetation plant functional types (PFTs) between 1865 and 2000. Between 1865 and 2000, the broadleaf

tree, needleleaf tree and shrub categories show a decline in global coverage with shrubs showing the largest decline (1404.1 Mha or -54.0 %) and needleleaf trees showing the smallest (218.5 Mha or -15.7 %). Both C3 and C4 grasses (which included agricultural crops and pastureland) show increases in global coverage of 1736.9 Mha (105.1 %) and 933.0 Mha (152.9 %) respectively. This reflects the general change in land patterns from the mid-19th century to the present day due to anthropogenic activity resulting in the replacement of forested regions by agricultural crops since the 1850s [*Ramankutty and Foley*, 1999; *Richards*, 1990; *Turner et al.*, 1993]. On a regional scale, changes in coverage of needleleaf tree (-150.7 Mha or -13.3 %), C3 grass (847.3 Mha or +134.7 %) and shrubs (-726.1 Mha or -59.8 %) are most pronounced over the northern hemisphere mid-latitude regions, with changes for broadleaf trees and C4 grasses largest over the tropics (-721.9 Mha (-24.3 %) and 548.4 Mha (+159.6 %)respectively). This change in broadleaf tree coverage over the tropics is of particular relevance, due to their role as large emitters of isoprene in the tropics [*Guenther et al.*, 2006].

2.5. Calculation of tropospheric ozone radiative forcing

We use the offline version of the *Edwards and Slingo* [1996] radiative transfer model to calculate the radiative effects of our simulated changes in tropospheric ozone [*Rap et al.*, 2015]. This model uses 6 bands in the shortwave, 9 bands in the longwave and a delta-Eddington 2 stream scattering solver at all wavelengths. The code uses monthly averaged climatology of temperature, water vapour and trace gases based upon the ECMWF re-analysis data. The resolution is 2.5° × 2.5° in the horizontal with 23 pressure levels in the vertical from the surface up to 1 hPa [*Rap et al.*, 2015]. Cloud and surface albedo data are compiled from the International Satellite Cloud Climatology Project (ISCCP)

archive [*Rossow and Schiffer*, 1999] and averaged over the time period 1983 to 2008. The calculated radiative forcing is the stratospherically adjusted radiative forcing defined as the change in net irradiance at the tropopause after allowing for the readjustment of stratospheric temperatures to radiative equilibrium whilst holding surface and tropospheric temperature and state variables (e.g. water vapour and cloud cover) fixed at the unperturbed values [*Myhre et al.*, 2013]. For the purpose of the offline radiative calculations only, stratospheric ozone (here we use the chemical tropopause definition based upon the 150 ppbv ozone concentration) is kept constant at present-day concentrations for each scenario during the radiative calculations, in order to isolate the radiative response to tropospheric ozone changes only.

3. Results and Discussion

3.1. Sensitivity of atmospheric chemistry-vegetation interactions to land cover and CO_2 changes

A number of key interactions dominate the expected response of atmospheric composition to changes in vegetation processes. Key effects are the response of dry deposition and isoprene emissions to vegetation cover changes and the impact of changing CO_2 on these processes. Land use change from the mid-19th century to the near present day involved the reduction in forest area and a replacement with large areas of cropland [*Ramankutty and Foley*, 1999; *Richards*, 1990]. This acted to reduce the rate of dry deposition [*Ganzeveld and Lelieveld*, 1995] of ozone and its precursors to the land surface and thus results in a local rise in concentrations. Further to this cropland species tend to emit lower amounts of isoprene which further contributes to a local increase in ozone concentrations, through a reduction in isoprene ozonolysis, and also acts to limit PAN formation.

This can reduce the long range transport of reactive nitrogen and thus lead to a drop in remote ozone concentrations away from the high isoprene sources. Further to this is the the effect of changing CO_2 concentrations which can reduce the rate of dry deposition by inducing stomatal closure. Finally, as discussed previously, higher CO_2 can also contribute to reduced isoprene emissions due to the inhibition effect. Figure 2 summarises the key chemical interactions between surface vegetation change and tropospheric ozone. The key determinants in how changes in isoprene emissions affect ozone both locally and in the remote troposphere are the presence or absence of NO_x, and the role of isoprene as a precursor for PAN formation. We discuss how these pathways are affected under each of our scenarios below.

3.1.1. Impact of vegetation and CO_2 changes on stomatal trace gas uptake

Figure 3 shows the changes in annual-mean stomatal conductance between each of the 4 model scenarios and the control simulation (PI_CTRL). Under the VEG_2000 scenario (Fig. 3a), stomatal conductances are lower in general than under the PI_CTRL scenario by up to 5.0×10^{-3} ms^{-1} ($\sim 20\,\%$), with a few locations seeing changes as high as 10.0×10^{-2} ms^{-1} ($\sim 100\,\%$). These largest differences are simulated over the northern hemisphere developed regions of North America, Europe and South East Asia, along with some tropical regions, which reflects locations of replacement of forests with crops and grasses (Table 2). The associated reduction in mean stomatal conductance in these regions is due to lower LAI and conductance rates over crop and grasslands compared to forested regions [*Ganzeveld and Lelieveld*, 1995].

Under the CO2_DDBVOC scenario (Fig. 3b) the model vegetation is exposed to a higher fixed present-day CO_2 mixing ratio of 368 ppmv compared to the lower mid-19th

century mixing ratio of 286 ppmv under the PI_CTRL scenario, resulting in the same reductions in stomatal conductance under both scenarios. This response is as expected due to higher CO_2 mixing ratios inducing stomatal closure in vegetation [*Gedney et al.*, 2006]. The largest differences are simulated over the tropical rainforest regions where stomatal conductances are up to 5.0×10^{-3} ms^{-1} ($\sim 20\,\%$) lower than under the PI_CTRL scenario. This largely reflects the geographical distribution of broadleaf tree species. However, widespread regions of North America, South East Asia and Europe see significant drops in stomatal conductance of up 2.0×10^{-3} ms^{-1} (around 12 %) under higher CO_{2Veg}. This reduction in stomatal conductance results in an overall reduction in the rate of dry deposition uptake of trace species under both scenarios when compared to the PI_CTRL scenario.

Under the CLIM_2000 (Fig. 3c) the reponse of stomatal conductances reflects both the changes in land use under the VEG_2000 scenario and the elevated CO_{2Veg} under the CO2_DDBVOC scenario. The large scale replacement of forests with cropland is evident over the northern hemisphere developed regions and the effect of the elevated CO_{2Veg} on reducing stomatal conductance is evident over the tropical rainforest regions. However, reductions in stomatal conductance are more widespread than seen under the VEG_2000 and CO2_DDBVOC scenarios with more regions showing reductions of 5.0×10^{-3} (20 %), with a few locations seeing changes as high as 10.0×10^{-2} ms^{-1} (($\sim 100\,\%$) E.g. over the Amazon rainforest.).

3.1.2. Impact of vegetation and CO_2 changes on isoprene emissions

Figure 4 shows the changes in annual mean isoprene emissions under the VEG_2000, CO2_DDBVOC and CLIM_2000 scenarios relative to the PI_CTRL scenario. Emissions

for the CO2_DD scenario are the same as those under the PI_CTRL scenario, since the higher CO_2 mixing ratio in this simulation only impacts dry deposition.

The replacement of high isoprene emitting broadleaf trees with grasses and crops under the VEG_2000 scenario leads to a reduction of 109 $TgCyr^{-1}$ in isoprene emissions compared with the PI_CTRL scenario emissions of 580 $TgCyr^{-1}$. Geographically, largest differences are in regions where broadleaf trees are replaced with crops and grasses, over the northern hemisphere developed regions and the tropics (Table 2). This reduction is consistent with, but slightly lower than the 1850–2000 land use change induced reduction in isoprene emissions of 135 $TgCyr^{-1}$ estimated by *Unger* [2014].

As discussed in previous studies [*Heald et al.*, 2009; *Pacifico et al.*, 2009; *Young et al.*, 2009; *Pacifico et al.*, 2012], higher CO_2 mixing ratios can result in the inhibition of isoprene emissions from vegetation. This is accounted for in the model photosynthesis-driven iBVOC scheme (See Section 2.1), and results in isoprene emissions of 456 $TgCyr^{-1}$ in the CO2_DDBVOC simulation, compared to 580 $TgCyr^{-1}$ in the PI_CTRL scenario. Largest differences in isoprene emissions due to the higher CO_{2Veg} are simulated over the tropical broadleaf forested regions where widespread regions show reductions in isoprene emissions of 1.0×10^{-10} $kgCm^{-2}s^{-1}$ ($\sim 19\,\%$), with maximum reductions of 2.8×10^{-9} $kgCm^{-2}s^{-1}$ (($\sim$ 22 %)) seen over the Amazon rainforest. Large reductions are also seen over widespread parts of North America, South East Asia and Europe where isoprene emissions are lower in the CO2_DDBVOC scenario by up to 4.0×10^{-11} $kgCm^{-2}s^{-1}$ ($\sim 20\,\%$). The reduction of -124 $TgCyr^{-1}$ in global isoprene emissions relative to the PI_CTRL simulation is slightly larger than that produced by the VEG_2000 scenario (-109 $TgCyr^{-1}$). The magnitude of this change is in agreement with the findings of *Pacifico et al.* [2012] who reported a similar

magnitude response (133 $TgCyr^{-1}$) using the same iBVOC scheme with present day and mid-19th century CO_2 mixing ratios. Under the CLIM_2000 scenario the reductions in isoprene emissions follow a similar pattern to those under the VEG_2000 scenario, but are more pronounced. This is due to the combination of the effects of vegetation change and CO_2 inhibition on isoprene emissions.

It should be noted, that large uncertainties exist in the CO_2 inhibition effect on isoprene emissions at the sub-ambient CO_2 concentrations of the 19th century. It has been shown in previous studies using limited plant species, that increasing CO_2 from a sub-ambient baseline (e.g. 240 ppmv), to present day concentrations (around 380–400 ppmv) produces mixed reponses dependant on plant species [*Wilkinson et al.*, 2009; *Possell et al.*, 2005]. This will thus introduce uncertainties in the responses of isoprene emissions to the change in CO_2 simulated in this study for 1865. However, despite these mixed reposnses and limited data for sub-ambient CO_2, a consistent picture is emerging that rise in CO_2 since the mid-19th century in general leads to a decrease in the isoprene emissions rate [*Possell et al.*, 2005; *Wilkinson et al.*, 2009].

The effect of CO_2 inhibition and land cover induced changes in isoprene emissions on tropospheric ozone is sensitive to the magnitude and distribution of emissions of NO_x. Under conditions of low NO_x abundance, isoprene may act as a net sink for tropospheric ozone [*Barket et al.*, 2004; *Pacifico et al.*, 2009]. This occurs where the direct reaction of ozone with isoprene becomes competitive with ozone production resulting from reaction of NO with peroxy radicals produced during isoprene oxidation. Global surface emissions of NO_x in our 1865 simulations are approximately a factor 4 lower than in present day (34.3 $TgNO_xyr^{-1}$ compared to 138.1 $TgNO_xyr^{-1}$)). The result is that many regions in

which an increase in isoprene results in net ozone production in present day, instead see a net ozone loss. We discuss these effects further in the following section.

3.2. Sensitivity of mid-19th century tropospheric composition to vegetation and CO_2 changes

3.2.1. 1865 to 2000 vegetation change VEG_2000 vs. PI_CTRL

Figure 5 shows the response of annual mean surface and annual zonal mean ozone and PAN concentrations to land cover change between 1865 and 2000, under mid-19th century surface emissions and climate. Surface ozone concentrations under the VEG_2000 simulation are up to 2 ppbv greater over parts of North America, South East Asia, South America and Africa compared to the mid-19th century control scenario, corresponding to regions of greatest loss of tree cover, and replacement with grass type vegetation (Table 2). This increase in surface ozone can be attributed to 2 different influences. Firstly, a reduction in stomatal conductance over these locations (Figure 3) leads to a reduction in the rate of dry deposition of ozone and its precursor species (e.g. NO_2 and PAN) to the land surface. This results in an increase in surface ozone concentrations. Secondly, the transition from broadleaf tree PFT type to grasses leads to a reduction is isoprene emissions which acts to further increase surface ozone concentrations. This is because despite the reduction in isoprene emissions, the reduction in PAN formation leads to elevated local NO_x concentrations which reacts readily with available isoprene in the region, which leads to enhanced local ozone production. Furthermore, the reduction in isoprene emissions in the overall low NO_x 1865 environment, reduces the direct reaction between ozone and isoprene further contributing to higher ozone concentrations.

In contrast, away from isoprene source regions, ozone concentrations under the VEG_2000 scenario are lower than under the PI_CTRL simulation by up to 1.5 ppbv (e.g. northern Africa, central Asia and Australia). Lower concentrations are also simulated over the oceans of at least 0.4 ppbv, with reductions of up to 2 ppbv over the tropical oceans. Under the VEG_2000 scenario, PAN mixing ratios are reduced compared with those in the PI_CTRL scenario by 50 pptv or greater over large parts of the continental land masses. As reductions in isoprene emissions over the northern hemisphere and tropical continents (Figure 4) are co-located with areas of greatest surface mid-19th century NO_x emissions (Figure 1), lower isoprene results in a substantial reduction in formation of PAN. This reduction in PAN formation in the VEG_2000 simulation leads to reduced transport of reactive nitrogen to the remote marine locations, and a consequent reduction in remote tropospheric ozone formation. This effect is evident in Fig. 6 where surface NO_x concentrations are lower under the VEG_2000 scenario by at least 10 pptv with mixing ratio reductions of up to 20 pptv over the tropical marine regions. Over the continents, NO_x mixing ratios are higher under the VEG_2000 scenario by values of 50pptv or higher in correspondance to the regions where the effects of reduced dry deposition lead to a net local increase in NO_x. This also contributes to the higher ozone values seen in these regions under the VEG_2000 scenario.

The impact of the lower isoprene emissions under the VEG_2000 scenario on free tropospheric ozone is evident in Figure 5. Modelled ozone concentrations are generally lower than under the PI_CTRL scenario by 0.4 ppbv to 0.8 ppbv throughout the free troposphere. Larger differences of around 1 ppbv are seen near the surface through the northern hemisphere tropics, and reductions in ozone concentrations of 2–6 ppbv are simulated in the

upper troposphere lower stratosphere (UTLS) region over the tropics of both hemispheres. These ozone reductions also result from reductions in PAN transport into the free troposphere under the VEG_2000 scenario. PAN concentrations are homogeneously lower throughout the entire troposphere by at least 4 pptv (10 %) with the largest differences seen in the northern hemisphere free troposphere where concentrations are up to 50 pptv lower (20 %, Fig. 5d). The extent of the ozone and PAN reductions in the upper northern hemisphere free troposphere, particularly over the tropics, highlight the importance of efficient vertical tranport in this region due to deep tropical convection (see schematic Fig .2). As shown in Sections 3.2.2 and 3.2.3, changes in PAN concentrations (Figures 7d and 8d) demonstrate that isoprene emissions changes have the dominant impact on upper tropospheric PAN and ozone (more so than dry deposition changes). This supports our assertion that these changes in tropical isoprene have widespread impacts on reative nitrogen and ozone in the free troposphere. Contributing to this are larger non-anthropogenic annual emissions of NO_x in the tropical regions (Figure 1) from sources including lightning, biomass burning and soil emissions.

Once transported to the upper troposphere (UT), the PAN lifetime increases as it becomes stable in the cold UT temperatures, where it is transported poleward in the global Hadley circulation. Consequently, changes in the rate of PAN formation from isoprene emission changes in the tropics have impacts on reactive nitrogen abundances, and hence our simulated ozone, throughout the global troposphere, particularly under the mid-19th century emissions scenario, where other sources of PAN (e.g. from mid-latitude anthropogenic emissions) are absent or substantially lower.

3.2.2. Ozone sensitivity to CO_2 impacts on dry deposition only (CO2_DD vs. PI_CTRL)

Figure 7c shows the differences in annual mean ozone and PAN concentrations between the CO2_DD and PI_CTRL scenarios. Dry deposition is suppressed due to reduced stomatal conductance under a higher CO_2 mixing ratio in the CO2_DD simulation. Consequently, ozone concentrations increase compared to those in the PI_CTRL scenario. In the southern hemisphere, largest differences are simulated over the Amazon and central parts of Africa, where ozone concentrations are up to 1 ppbv greater than under the PI_CTRL scenario. This effect is due to the high coverage of broadleaf trees and high rates of photosynthesis, resulting in a strong CO_2 flux into vegetation. These regions show the largest response to the higher CO_2 mixing ratio and hence the largest reponse in stomatal conductance. Surface ozone concentrations are greater by at least 0.2 ppbv throughout the majority of the northern hemisphere and up to 1 ppbv over eastern parts of the United States, Europe and south eastern parts of Asia. The lower rates of ozone deposition lead to homogeneously higher ozone concentrations throughout the free troposphere under the CO2_DD scenario by at least 0.1 ppbv.

Dry deposition is also an important sink for PAN and NO_2, leading to enhanced PAN mixing ratios under the CO2_DD scenario. Largest differences are simulated over the Amazon and central Africa in the southern hemisphere (10–20 pptv) and over widespread regions of North America, Europe and eastern Siberia in the northern hemisphere where differences are 20 pptv or larger, with consequent impacts on remote tropospheric ozone, as discussed in the previous section. As a result of these higher PAN mixing ratios, more NO_x is locked up as PAN, resulting in slightly lower NO_x mixing ratios under the

CO2_DD scenario with the greatest reductions of 10 pptv seen over South America and Central Africa (Fig. 6).

3.2.3. Ozone sensitivity to combined CO_2 impacts on dry deposition and isoprene emissions (CO2_DDBVOC vs. PI_CTRL)

The combined effects of reduced rates of dry deposition and isoprene emissions under the CO2_DDBVOC scenario compared with PI_CTRL are shown in Figure 8. These effects result in an almost universal increase in surface ozone concentrations over the NH and tropical continents. These increases in surface ozone show a similar spatial pattern to those simulated in the CO2_DD scenario, but are more pronounced in regions of strong isoprene emission, and more widespread through the northern hemisphere. The CO_2 inhibition of isoprene emissions in the CO2_DDBVOC scenario acts to reduce isoprene emissions globally in all regions (Fig. 4). The uniform increase in surface ozone in NH continental regions is consistent with isoprene acting as a net ozone sink in these regions under low mid-19th century NO_x emissions, but it is also partly a response to less efficient dry deposition under enhanced CO_2 concentrations.

Surface ozone mixing ratios are lower under the CO2_DDBVOC scenario over the remote regions with differences approaching 1 ppbv over the tropical Atlantic. This response is similar to that shown in the VEG_2000 scenario, and is a result of reduced PAN formation in tropical regions under reduced isoprene emissions. This leads to lower PAN and NO_2 abundances and ozone production rates over the remote marine regions. Figure 8 shows reductions in PAN mixing ratios under the CO2_DDBVOC scenario compared with PI_CTRL. Largest differences are simulated over parts of North America, Europe, South America and central Africa where PAN concentrations are up to 40 pptv lower.

PAN reductions are smaller than those produced under the VEG_2000 scenario (Fig. 5). This is because CO_2-induced reductions in dry deposition enhance PAN concentrations which subsequently partially offset the reduced PAN formation as a result of the lower isoprene emissions. Different spatial patterns and magnitudes of isoprene emission reductions produced by the change in vegetation compared to the change in global CO_2 mixing ratio (Fig. 4), also play a role in these different responses. The response in surface NO_x concentrations (Fig. 6)d shows a similar pattern to that from the VEG_2000 scenario, however the increases in NO_x concentrations over the land masses are much less pronounced at around 30 pptv compared to 50 pptv or larger under the VEG_2000 scenario. Over the remote marine regions, NO_x concentrations are seen to be lower under the CO2_DDBVOC scenario than under the PI_CTRL scenario due to reduced PAN formation, as discussed above. These changes in NO_x have consequent impacts on surface ozone concentrations as discussed in Section 3.2.1.

The more moderate reduction in PAN concentrations, than seen for the VEG_2000 scenario, also leads to contrasting zonal mean tropospheric ozone responses in each hemisphere. In the southern hemisphere, ozone reduces under the CO2_DDBVOC scenario by 0.1–0.2 ppbv due to the PAN-induced reduction in ozone formation over the remote marine areas. In the northern hemisphere (NH), ozone increases at high latitudes and in the free troposphere. Again, this is a consequence of the combined reductions in dry deposition and isoprene emissions under enhanced CO_2. Over the northern hemisphere continents, isoprene acts as an ozone sink, and the larger proportion of land mass in the northern hemisphere also results in a large reduction in dry deposition loss of ozone and its precursors. For this scenario in the NH, these effects dominate over the effects of a reduc-

tion in PAN due to lower isoprene emissions, which caused substantial free tropospheric ozone reductions in the VEG_2000 scenario.

3.2.4. Impacts of model climate (CLIM_2000 vs. PI_CTRL)

Figure 9 compares annual mean ozone and PAN concentrations between the PI_CTRL and the CLIM_2000 scenario. These differences include the effects of both vegetation change and CO_2 increase on dry deposition and isoprene emissions, as well as the effects of the changes in SSTs, sea-ice fields and greenhouse gas concentrations between 1860 and 2000. These changes all combine to produce increases in surface ozone in the CLIM_2000 simulation over most of the northern hemisphere and tropical SH continents, and ozone decreases over the remote SH oceans. Ozone increases are as much as 5 ppbv over parts of North America and the North Atlantic, and at least 1 ppbv in most NH continental regions. In the tropics and southern hemisphere, ozone increases and decreases are co-located with isoprene emission reductions and increases respectively (Fig. 4), due to the ozone sink effect of isoprene under low NO_x. Ozone mixing ratios are greater under the CLIM_2000 scenario by at least 2 ppbv throughout the northern hemisphere free troposphere, with differences of up to 6–8 ppbv in the mid-latitude upper troposphere.

The increases in NH continental surface ozone simulated in the CLIM_2000 simulation relative to the PI_CTRL scenario are more substantial than under any of the other scenarios. This is mainly due to the effects of the change in climate on stomatal conductance (Figure 3) producing substantial reductions in dry deposition velocities, compounding the effects of CO_2 increases and land cover change over many regions. In addition climate impacts on circulation, atmospheric kinetics and lightning emissions could also contribute to these large ozone changes. Large differences in stratospheric ozone are simulated, since

the CLIM_2000 simulation uses prescribed stratospheric ozone representative of the driving climate of year 2000, which is lower than that for a mid-19th century atmosphere (PI_CTRL scenario). The effects of climate change and isoprene emission reductions have substantial impacts on PAN in the CLIM_2000 simulation, where large reductions are simulated at the surface over the continents and throughout the troposphere. These are larger than under any other scenario which could also be the reason why ozone changes are largest under CLIM_2000. The strong temperature dependence of the PAN lifetime [*Singh*, 1987] means that under warmer present-day climate conditions its tropospheric loss rate is enhanced. This effect acts to enhance the effects of reductions in isoprene emissions under enhanced CO_2 and vegetation change to produce larger PAN decreases throughout the troposphere. Figure 6 shows that the influence of the PAN reductions on surface NO_x concentrations follows a similar pattern to that seen under the VEG_2000 scenario, due to the effects of reduced isoprene emissions and PAN formation as discussed in Sect. 3.2.1. This results in 2 different effects dependant on location. Under the 1865 emissions scenario, areas over land are typically in a low NO_x environment and therefore the enhancement of surface NO_x concentrations (Fig. 6) combine with the effects of reduced dry deposition and reduced isoprene emissions to lead to enhancements of surface ozone concentrations. This could be an additional reason for the rise in modelled surface ozone due to the change in model climate between the CLIM_2000 and PI_CTRL scenarios, an effect shown in previous studies [*Jacob and Winner*, 2009; *Fiore et al.*, 2012]. In contrast, the effects of reduced PAN concentrations result in large reductions in ozone in the remote SH and tropics of up to 4 ppbv. Ozone reductions in regions remote from NO_x

sources are also enhanced by larger water vapour abundances in the present-day climate of the CLIM_2000 simulation.

The effect of CO_2 fertilistation on vegetation likely also contributes to the larger tropospheric ozone concentrations under the CLIM_2000 scenario. As recently suggested by [*Wu et al.*, 2012; *Tai et al.*, 2014] higher CO_2 can enhance plant productivity increasing LAI, and thus change dry deposition and bVOC emissions, which in the future may have comparable impacts on ozone concentrations as the changing climate itself. As leaf phenology is determined online in our simulations using TRIFFID, and the CLIM_2000 scenario is driven using a higher CO_2 concentration representative of the near present day, the changes in LAI will include the impacts of CO_2 fertilisation. Therefore the response of ozone concentrations CO_2-driven LAI increase will be included in this scenario, however we have not isolated it explicitly in this study.

4. Impacts of changing atmospheric chemistry-vegetation interactions on free tropospheric ozone distributions and implications for radiative effect

Our simulations show that the sensitivities of mid-19th century ozone to changes in the vegetation cover only and to changes in CO_{2Veg} are of similar magnitude, but of opposite sign in terms of their effects on high latitude and tropical mid-tropospheric ozone. The effects of increasing CO_2 on stomatal conductance and on isoprene emissions both produce increases in continental surface ozone concentrations, due to a reduction in the deposition sink and isoprene ozonolysis sink of ozone. The effects of the reduced isoprene on PAN concentrations are larger and opposite in sign to the impacts of the CO_2 reduction in dry deposition, resulting in reduced PAN transport to remote regions and less ozone production. This effect also produces a large reduction in tropical UT ozone in response

to both the land cover and CO_2 changes. Combining these changes in land cover and CO_2 with changes in climate between mid-19th century and present day produces increases in tropospheric ozone, and the largest increases in surface ozone throughout the northern hemisphere. This is a combined response to CO_2-induced and land-cover-induced changes in isoprene emissions, reducing the isoprene ozonolysis ozone sink over the continents, and climate-driven reductions in stomatal conductance compounding reductions due to CO_2 increases. This results in further reduction in the dry deposition sink.

The changes in the tropospheric ozone burden between each of our scenarios and the PI_CTRL simulation is shown in Table 3. The simulations indicate a change in the modelled ozone burden of between -3.3 Tg (1.6 %) under the VEG_2000 scenario to 1.3 Tg (0.6 %) under the CLIM_2000 scenario. Using interannual standard deviation from our model runs, we estimate a range in variability on our estimates of the troposheric ozone burden of between 8.7 Tg (4.4 %) for the VEG_2000 scenario to 10.9 Tg (5.3 %) for the CO2_DDBVOC scenario. Overall this shows that the sensitivities of tropospheric ozone (in the mid-19th century) to different treatments of atmospheric chemistry-vegetation interactions is smaller than the inter-annual variability. In this study we have shown that uncertainties arising from assumptions regarding the represenations of atmopheric chemisty-vegetation can add to this variability in our best estimate of atmospheric conditions in the mid-19th century which further stresses the case for better representation of these processes in Earth-system models.

To put our work into context of previous studies, we also calculated our best estimate of the change in tropospheric ozone burden between the mid-19th century and the present day (PI_CTRL vs. PD_2000 scenarios), which is 89.2 Tg (43.7 %). This is consistent

with previous work which estimated the mid-19th century to present day change in ozone burden at 71.0–130.0 Tg [*Lamarque et al.*, 2005] and slightly higher than the ACCMIP study which estimated a modelled change in ozone burden of approximately 30 % since 1850 [*Young et al.*, 2013]. Figure 10 shows the annually- and zonally-averaged changes in ozone between the PI_CTRL scenario and the present day atmosphere (PD_2000). Ozone is shown to increase by at least 50 % (around 12 ppbv) throughout the northern hemisphere between the mid-19th century and the present day. These increases approach 80–90 % (around 18–20 ppbv) in the lower to mid northern hemisphere troposphere with an approximate doubling of ozone seen at the surface between 30N and 60N. In the southern hemisphere ozone concentrations are shown to increase by 10–40 % (2–5 ppbv) under all scenarios with the greatest changes seen around the tropics. In the upper troposphere, ozone increases are at least 10 % (2, ppbv), with the greatest changes seen around the tropopause between 20N and 30N. The changes in this region are around 50 % (16 ppbv). This is in agreement with recent results from ACCMIP [*Young et al.*, 2013] which showed mid-19th century to present day increases in tropospheric ozone of 5–20 ppbv in the lower troposphere in the northern hemisphere, 10-20 ppbv in the upper tropical troposphere and 2–10 ppbv throughout the southern hemisphere troposphere.

Our best estimate for the tropospheric ozone radiative forcing (PD_2000 - PI_CTRL) is 0.264 W m^{-2}. This falls towards the lower end of previous estimates: 0.25–0.45 W m^{-2} by *Gauss et al.* [2006], 0.44 $\pm$ 0.13 W m^{-2} by *Skeie et al.* [2011], 0.29–0.53 W m^{-2} by the ACCMIP model intercomparison project [*Stevenson et al.*, 2013], 0.2–0.6 W m^{-2} by *Myhre et al.* [2013], and 0.32 W m^{-2} by *Rap et al.* [2015]. Our lower estimate could be due to the assumptions made regarding the prescribed anthropogenic emissions, as discussed further

below. We also find some sensitivity of our forcing to the tropopause definition. Our choice of the 150 ppbv ozone contour to define the chemical tropopause means that some negative changes in lower stratospheric ozone between mid-19th century and present day are included contributing to a damping of our tropospheric forcing estimate. However, this damping effect has been shown to be relatively small (approximately 5 %) [*Stevenson et al.*, 2013].

To isolate the effect of mid-19th century to present day change in vegetation on the tropospheric ozone radiative effect, we calculate the difference between the ozone radiative effects in the PI_CTRL and the VEG_2000 simulations. We find a -0.012 W m^{-2} trospospheric ozone radiative effect from using present day land cover in the VEG_2000 scenario compared to the PI_CTRL scenario (Table 4). Thus, our results imply a negative impact on the tropospheric ozone radiative effect of -0.012 W m^{-2} (Table 4) due to this change. This sensitivity is an order of magnitude smaller than the negative tropospheric ozone effect of -0.13 W m^{-2} attributed to reductions in vegetation cover since the mid-19th century by *Unger* [2014]. While the definition of the quantity calculated here is different from that of *Unger* [2014], the difference demonstrates the importance of experimental design in derivation of this sensitivity. The key difference between the definitions is the assumption regarding precursor emissions (particularly NO_x) from anthropogenic sources. Our radiative effect is calculated based on a change in vegetation from PI to year 2000, with emissions fixed at PI values. The previous estimate from *Unger* [2014] calculated the ozone forcing due to changes in land cover between PI and present day, using present day emissions. The response of ozone and the associated radiative sensitivity is smaller

in our simulations due to the land cover-induced changes in isoprene emissions occurring in lower NO_x conditions (see schematic Fig. 2).

As NO_x emissions have varied dynamically between 1865 and 2000, our results coupled with those of *Unger* [2014] suggest that a shift to a higher NO_x regime over that periods means that sensitivities of the tropospheric ozone radiative effect to vegetation cover have likely increased by an order of magnitude. Overall, our simulations show that it is important to use the correct baseline land cover and that ideally simulated vegetation processes must also change interactively with dynamically changing NO_x emissions.

Our results highlight that the ozone radiative effect response to land cover change is dominated by the impacts of isoprene emission change on ozone in the upper troposphere, consistent with other studies which showed the importance of the tropical tropopause region [*Worden et al.*, 2011; *Riese et al.*, 2012; *Rap et al.*, 2015]. This response is largely controlled by the availability of NO_x, and processes that transport ozone and precursors to the upper troposphere. A key factor is the formation of PAN from isoprene oxidation and its transport to the tropical UT. The radiative impacts of ozone changes produced by the effects of changing CO_2 on isoprene emissions and dry deposition (CO_{2Veg}) between PI and present-day (CO2_DDBVOC - PI_CTRL and CO2_DD - PI_CTRL) are very small (both 0.001 W m^{-2}). This is due to their much smaller impacts on ozone in the upper troposphere (Figs. 7 and 8). It is however noted here that the relative sensitivity of the overall radiative forcing to changes in atmospheric chemistry-vegetation interactions is much smaller than the value of the forcing itself (0.264 W m^{-2}) with the largest contribution to this forcing coming from changes in anthropogenic emissions since 1865 [*Stevenson et al.*, 2013].

Previous studies have also noted the sensitivity of tropospheric ozone forcing to changes in natural emissions. *Mickley et al.* [2001] found that by increasing emissions of BVOCs from vegetation by 50 % and increasing NO_x emissions from soil and lightning, an instantaneous forcing of 0.72–0.80 W m^{-2} was calculated. This was approximately double the value of their standard mid-19th century simulation (0.44 W m^{-2}). Finally, uncertainties in biomass burning of NO_x in the mid-19th century along with potential uncertainties in soil emissions also lead to uncertainty in the mid-19th century tropospheric ozone burden. This may be particularly important, given the role of PAN in determining the response of remote surface and free tropospheric ozone to changes in isoprene emissions that we have highlighted. As the focus of this work is to isolate the effects of changing vegetation on isoprene emissions and dry deposition processes we did not explicitly test the response to changing biomass burning and soil NO_x emissions. However, we expect our results to also be sensitive to our assumption of mid-19th century biomass burning [*Pacifico et al.*, 2015; *Rap et al.*, 2015] and soil emissions of NO_x. This should be the subject of further investigation in future studies.

5. Conclusions

In this study, simulations using an Earth System Model showed that changes in dry deposition and isoprene emissions due to vegetation change (1865 to 2000) are shown to have a larger effect on surface ozone and the ozone burden (a 1.6 % burden reduction from a control simulation) than those associated with the effects of the mid-19th century to present-day change in atmospheric CO_2 concentration on isoprene emissions and dry deposition (a 0.4 % burden increase from the control simulation). Our results also show that the response of ozone concentrations to vegetation and CO_2 changes is dominated by

the impacts of changing isoprene emissions rather than changing dry deposition, agreeing with previous work [*Lamarque et al.*, 2005], in the low NO_x regime of the mid-19th century period.

Changes in surface vegetation cover since the mid-19th century, and CO_2 suppression of isoprene emissions under present-day compared with mid-19th century lead to decreases in global isoprene emissions of 19% and 21% respectively. The effect of land-cover driven decreases in isoprene since mid-19th century is to increase surface ozone concentrations over the vegetated continents by up to 2 ppbv. The same decreases in isoprene result in lower surface ozone concentrations over non-vegetated and marine regions, due to decreased PAN formation and the subsequent decrease in transport of NO_x to these regions, reducing ozone formation. When the land cover and CO_2 changes are combined with a change in model climate, the ozone burden increases by 0.6 % and surface ozone concentrations increase by up to 5 ppbv compared to the control simulation, with increases of 6-8 ppbv in the mid-latitude upper troposphere.

Our simulations show that our best estimate of the mid-19th century troposheric ozone burden is 203.7±9.4 Tg. We show that depending on assumptions regarding the model land PFT distribution, the atmospheric CO_2 mixing ratio controlling vegetation stomatal conductance and isoprene emission, and the model climate, that this value can increase to 205.0±9.2 Tg or be as low as 200.4±8.8 Tg. The associated mid-19th century to present day change in ozone burden (present day burden of 292.9±18.4 Tg) is 89.2 Tg which leads to an associated radiative forcing of 0.264 W m^{-2}. Overall, the change in vegetation only (VEG_2000 - PI_CTRL) produces the largest differences (with reference to the control simulation) at the tropopause level resulting in a negative radiative forcing of -0.012 W

m^{-2}. Changes in vegetation CO_2 exposure produce a much smaller impact at tropopause level, leading to a small radiative effect of $+0.001\,W\,m^{-2}$.

Our results highlight the sensitivity of both the mid-19th century surface ozone distribution and tropospheric ozone burden to assumptions regarding atmospheric chemistry-vegetation interactions, in particular isoprene emissions and their interaction with emissions of NO_x. Further work is required to understand how uncertainties in our knowledge of mid-19th century NO_x emissions interact with the sensitivities to vegetation cover presented here, and the subsequent impacts on simulating PI ozone and ozone radiative forcing.

Acknowledgments. This work was supported with funding from the UK Natural Environment Research Council (NERC) (NE/G523755/1) and the UK Met Office as a CASE studentship. We acknowledge use of the MONSooN system, a collaborative facility supplied under the Joint Weather and Climate Research Programme, a strategic partnership between the Met Office and the Natural Environment Research Council. All model data used in the analysis is available on request from the corresponding author (S.Arnold@leeds.ac.uk).

References

Anenberg, S. C., L. W. Horowitz, D. Q. Tong, and J. J. West (2010), An Estimate of the Global Burden of Anthropogenic Ozone and Fine Particulate Matter on Premature Human Mortality Using Atmospheric Modeling, *Environmental Health Perpectives*, *118*(9), 1189–1195, doi:10.1289/ehp.0901220.

Arneth, A., U. Niinemets, S. Pressley, J. Bäck, P. Hari, T. Karl, S. Noe, I. C. Prentice, D. Serça, T. Hickler, A. Wolf, and B. Smith (2007), Process-based estimates of terrestrial ecosystem isoprene emissions: incorporating the effects of a direct co¡sub¿2¡/sub¿-isoprene interaction, *Atmospheric Chemistry and Physics*, *7*(1), 31–53, doi:10.5194/acp-7-31-2007.

Avnery, S., D. L. Mauzerall, and A. M. Fiore (2013), Increasing global agricultural production by reducing ozone damages via methane emission controls and ozone-resistant cultivar selection, *Global Change Biology*, *19*(4), 1285–1299, doi:10.1111/gcb.12118.

Barket, D., J. Grossenbacher, J. Hurst, P. Shepson, K. Olszyna, T. Thornberry, M. Carroll, J. Roberts, C. Stroud, J. Bottenheim, and T. Biesenthal (2004), A study of the NOx dependence of isoprene oxidation, *Journal of Geophysical Research: Atmospheres*, *109*(D11), doi:10.1029/2003JD003965.

Collins, W. J., S. Sitch, and O. Boucher (2010), How vegetation impacts affect climate metrics for ozone precursors, *Journal of Geophysical Research: Atmospheres*, *115*(D23), doi:10.1029/2010JD014187.

Collins, W. J., N. Bellouin, M. Doutriaux-Boucher, N. Gedney, P. Halloran, T. Hinton, J. Hughes, C. D. Jones, M. Joshi, S. Liddicoat, G. Martin, F. O'Connor, J. Rae, C. Senior, S. Sitch, I. Totterdell, A. Wiltshire, and S. Woodward (2011), Development and evaluation of an Earth-System model - HadGEM2, *Geoscientific Model Development*, *4*(4), 1051–1075, doi:10.5194/gmd-4-1051-2011.

Edwards, J. M., and A. Slingo (1996), Studies with a flexible new radiation code .1. choosing a configuration for a large-scale model, *Quarterly Journal Of The Royal Meteorological Society*, *122*(531), 689–719, doi:10.1002/qj.49712253107.

Essery, R. L. H., M. J. Best, R. A. Betts, P. M. Cox, and C. M. Taylor (2003), Explicit representation of subgrid heterogeneity in a GCM land surface scheme, *Journal Of Hydrometeorology*, *4*(3), 530–543, doi:10.1175/1525-7541(2003)004¡0530:EROSHI¿2.0.CO;2.

Fiore, A. M., V. Naik, D. V. Spracklen, A. Steiner, N. Unger, M. Prather, D. Bergmann, P. J. Cameron-Smith, I. Cionni, W. J. Collins, S. Dalsoren, V. Eyring, G. A. Folberth, P. Ginoux, L. W. Horowitz, B. Josse, J.-F. Lamarque, I. A. MacKenzie, T. Nagashima, F. M. O'Connor, M. Righi, S. T. Rumbold, D. T. Shindell, R. B. Skeie, K. Sudo, S. Szopa, T. Takemura, and G. Zeng (2012), Global air quality and climate, *Chemical Society Reviews*, *41*(19), 6663–6683, doi:10.1039/c2cs35095e.

Folberth, G., D. Hauglustaine, J. Lathiere, and F. Brocheton (2006), Interactive chemistry in the Laboratoire de Meteorologie Dynamique general circulation model: model descirption and impact analysis of biogenic hydrocarbons on tropsopheric chemistry, *Atmospheric Chemistry And Physics*, *6*, 2273–2319, doi:10.5194/acp-6-2273-2006.

Fu, Y., and A. P. K. Tai (2015), Impact of climate and land cover changes on tropospheric ozone air quality and public health in east asia between 1980 and 2010, *Atmospheric Chemistry and Physics*, *15*(17), 10,093–10,106, doi:10.5194/acp-15-10093-2015.

Ganzeveld, L., and J. Lelieveld (1995), Dry deposition parameterization in a chemistry general circulation model and its influence on the distribution of reactive trace gases, *Journal of Geophysical Research - Atmospheres*, *100*, 20,999–21,012.

Gauss, M., G. Myhre, I. S. A. Isaksen, V. Grewe, G. Pitari, O. Wild, W. J. Collins, F. J. Dentener, K. Ellingsen, L. K. Gohar, D. A. Hauglustaine, D. Iachetti, J. F. Lamarque, E. Mancini, L. J. Mickley, M. J. Prather, J. A. Pyle, M. G. Sanderson, K. P. Shine, D. S. Stevenson, K. Sudo, S. Szopa, and G. Zeng (2006), Radiative forcing since preindustrial

times due to ozone change in the troposphere and the lower stratosphere, *Atmospheric Chemistry And Physics*, *6*, 575–599, doi:10.5194/acp-6-575-2006.

Gedney, N., P. Cox, R. Betts, O. Boucher, C. Huntingford, and P. Stott (2006), Detection of a direct carbon dioxide effect in continental river runoff records, *Nature*, *439*, 835–838, doi:10.1038/nature04504.

Giannakopoulos, C., T. P. Chipperfield, K. S. Law, and J. A. Pyle (1999), Validation and intercomparison of wet and dry deposition schemes using Pb-210 in a global three-dimensional off-line chemical transport model, *Journal Of Geophysical Research-Atmospheres*, *104*(D19), 23,761–23,784, doi:10.1029/1999JD900392.

Guenther, A., P. Zimmerman, P. Harley, R. Monson, and R. Fall (1993), Isoprene and monoterpene emission rate variability - model evaluations and sensitivity analyses, *Journal Of Geophysical Research-Atmospheres*, *98*(D7), 12,609–12,617, doi:10.1029/93JD00527.

Guenther, A., T. Karl, P. Harley, C. Wiedinmyer, P. Palmer, and C. Geron (2006), Estimates of global terrestrial isoprene emissions using MEGAN (Model of Emissions of Gases and Aerosols from Nature), *Atmospheric Chemistry And Physics*, *6*, 3181–3210, doi:10.5194/acp-6-3181-2006.

Hauglustaine, D. A., and G. P. Brasseur (2001), Evolution of tropospheric ozone under anthropogenic activities and associated radiative forcing of climate, *Journal Of Geophysical Research-Atmospheres*, *106*(D23), 32,337–32,360, doi:10.1029/2001JD900175.

Heald, C. L., M. J. Wilkinson, R. K. Monson, C. A. Alo, G. Wang, and A. Guenther (2009), Response of isoprene emission to ambient co_2 changes and implications for global budgets, *Global Change Biology*, *15*(5), 1127–1140, doi:10.1111/j.1365-2486.2008.01802.x.

Hollaway, M. J., S. R. Arnold, A. J. Challinor, and L. D. Emberson (2012), Intercontinental trans-boundary contributions to ozone-induced crop yield losses in the northern hemisphere, *Biogeosciences*, *9*(1), 271–292, doi:10.5194/bg-9-271-2012.

Hurtt, G. C., L. P. Chini, S. Frolking, R. A. Betts, J. Feddema, G. Fischer, J. P. Fisk, K. Hibbard, R. A. Houghton, A. Janetos, C. D. Jones, G. Kindermann, T. Kinoshita, K. K. Goldewijk, K. Riahi, E. Shevliakova, S. Smith, E. Stehfest, A. Thomson, P. Thornton, D. P. van Vuuren, and Y. P. Wang (2011), Harmonization of land-use scenarios for the period 1500-2100: 600 years of global gridded annual land-use transitions, wood harvest, and resulting secondary lands, *Climatic Change*, *109*(1-2, SI), 117–161, doi:10.1007/s10584-011-0153-2.

Jacob, D. J., and D. A. Winner (2009), Effect of climate change on air quality, *Atmospheric Environment*, *43*(1), 51 – 63, doi:http://dx.doi.org/10.1016/j.atmosenv.2008.09.051.

Jones, C. D., J. K. Hughes, N. Bellouin, S. C. Hardiman, G. S. Jones, J. Knight, S. Liddicoat, F. M. O'Connor, R. J. Andres, C. Bell, K.-O. Boo, A. Bozzo, N. Butchart, P. Cadule, K. D. Corbin, M. Doutriaux-Boucher, P. Friedlingstein, J. Gornall, L. Gray, P. R. Halloran, G. Hurtt, W. J. Ingram, J.-F. Lamarque, R. M. Law, M. Meinshausen, S. Osprey, E. J. Palin, L. Parsons Chini, T. Raddatz, M. G. Sanderson, A. A. Sellar, A. Schurer, P. Valdes, N. Wood, S. Woodward, M. Yoshioka, and M. Zerroukat (2011), The HadGEM2-ES implementation of CMIP5 centennial simulations, *Geoscientific Model Development*, *4*(3), 543–570, doi:10.5194/gmd-4-543-2011.

Klein Goldewijk, K., A. Beusen, and P. Janssen (2010), Long term dynamic modelling of global population and built-up area in a spatially explicit way: HYDE 3.1, *Holocene*, *20*, 565–573, doi:10.1177/0959683609356587.

Lamarque, J. F., P. Hess, L. Emmons, L. Buja, W. Washington, and C. Granier (2005), Tropospheric ozone evolution between 1890 and 1990, *Journal Of Geophysical Research-Atmospheres*, *110*(D8), D08,304, doi:10.1029/2004JD005537.

Lamarque, J. F., T. C. Bond, V. Eyring, C. Granier, A. Heil, Z. Klimont, D. Lee, C. Liousse, A. Mieville, B. Owen, M. G. Schultz, D. Shindell, S. J. Smith, E. Stehfest, J. Van Aardenne, O. R. Cooper, M. Kainuma, N. Mahowald, J. R. McConnell, V. Naik, K. Riahi, and D. P. van Vuuren (2010), Historical (1850-2000) gridded anthropogenic and biomass burning emissions of reactive gases and aerosols: methodology and application, *Atmospheric Chemistry And Physics*, *10*(15), 7017–7039, doi:10.5194/acp-10-7017-2010.

Lelieveld, J., T. Butler, J. Crowley, T. Dillon, H. Fischer, L. Ganzeveld, H. Harder, M. Lawrence, M. Martinez, D. Taraborrelli, and J. Williams (2008), Atmospheric oxidation capacity sustained by a tropical forest, *Nature*, *452*, 737–740, doi:10.1038/nature06870.

Lombardozzi, D., J. P. Sparks, and G. Bonan (2013), Integrating o_3 influences on terrestrial processes: photosynthetic and stomatal response data available for regional and global modeling, *Biogeosciences*, *10*(11), 6815–6831, doi:10.5194/bg-10-6815-2013.

Lombardozzi, D., S. Levis, G. Bonan, P. G. Hess, and J. P. Sparks (2015), The Influence of Chronic Ozone Exposure on Global Carbon and Water Cycles, *Journal of Climate*, *28*(1), 292–305, doi:10.1175/JCLI-D-14-00223.1.

Loveland, T., B. Reed, J. Brown, D. Ohlen, Z. Zhu, L. Yang, and J. Merchant (2000), Development of a global land cover characteristics database and IGBP DISCover from 1km AVHRR data, *International Journal of Remote Sensing*, *21*, 1303–1330, doi:

10.1080/014311600210191.

Mickley, L. J., D. J. Jacob, and D. Rind (2001), Uncertainty in preindustrial abundance of tropospheric ozone: Implications for radiative forcing calculations, *Journal Of Geophysical Research-Atmospheres*, *106*(D4), 3389–3399, doi:10.1029/2000JD900594.

Monson, R., and R. Fall (1989), Isoprene emission from Aspen leaves - influence of environment and relation to photosynthesis and photorespiration, *Plant Physiology*, *90*(1), 267–274, doi:10.1104/pp.90.1.267.

Monson, R. K., N. Trahan, T. N. Rosenstiel, P. Veres, D. Moore, M. Wilkinson, R. J. Norby, A. Volder, M. G. Tjoelker, D. D. Briske, D. F. Karnosky, and R. Fall (2007), Isoprene emission from terrestrial ecosystems in response to global change: minding the gap between models and observations, *Philosophical Transactions Of The Royal Society A-Mathematical Physical And Engineering Sciences*, *365*(1856), 1677–1695, doi:10.1098/rsta.2007.2038.

Moxim, W. J., H. Levy, and P. S. Kasibhatla (1996), Simulated global tropospheric PAN: Its transport and impact on no_x, *Journal Of Geophysical Research-Atmospheres*, *101*(D7), 12,621–12,638, doi:10.1029/96JD00338.

Myhre, G., D. Shindell, F. M. Breon, W. Collins, J. Fuglestvedt, J. Huang, D. Koch, J. F. Lamarque, D. Lee, B. Mendoza, T. Nakajima, A. Robock, G. Stephens, T. Takemura, and H. Zhang (2013), Anthropogenic and Natural Radiative Forcing, in *Climate Change 2013: The Physical Science Basis. Contribution of Working Group I to the Fifth Assessment Report of the Intergovernmental Panel on Climate Change*, edited by T. Stocker, D. Qin, G. K. Plattner, M. Tignor, S. Allen, J. Boschnung, A. Nauels, Y. Xia, V. Bex, and P. Midgley, Cambridge University Press, Cambridge, United Kingdom and New

York, NY, USA.

Niinemets, U., and Z. Sun (2015), How light, temperature, and measurement and growth [CO2] interactively control isoprene emission in hybrid aspen, *Journal of Experimental Botany*, *66*(3), 841–851, doi:10.1093/jxb/eru443.

Niinemets, U., J. Tenhunen, P. Harley, and R. Steinbrecher (1999), A model of isoprene emission based on energetic requirements for isoprene synthesis and leaf photosynthetic properties for *Liquidambar and Quercus*, *Plant, Cell and Environment*, *22*, 1319–1335, doi:10.1046/j.1365-3040.1999.00505.x.

Niinemets, U., A. Arneth, U. Kuhn, R. Monson, and M. Penuelas, J. ad Staudt (2010a), The emission factor of volatile isoprenoids: stress, acclimation, and developmental responses, *Biogeosciences*, *7*(7), 2203–2223, doi:10.5194/bg-7-2203-2010.

Niinemets, U., R. K. Monson, A. Arneth, P. Ciccioli, J. Kesselmeier, U. Kuhn, S. M. Noe, J. Penuelas, and M. Staudt (2010b), The leaf-level emission factor of volatile isoprenoids: caveats, model algorithms, response shapes and scaling, *Biogeosciences*, *7*(6), 1809–1832, doi:10.5194/bg-7-1809-2010.

O'Connor, F. M., C. E. Johnson, O. Morgenstern, N. L. Abraham, P. Braesicke, M. Dalvi, G. A. Folberth, M. G. Sanderson, P. J. Telford, A. Voulgarakis, P. J. Young, G. Zeng, W. J. Collins, and J. A. Pyle (2014), Evaluation of the new ukca climate-composition model part 2: The troposphere, *Geoscientific Model Development*, *7*(1), 41–91, doi:10.5194/gmd-7-41-2014.

Pacifico, F., S. Harrison, C. Jones, and S. Sitch (2009), Isoprene emissions and climate, *Atmospheric Environment*, *43*(39), 6121–6135, doi:http://dx.doi.org/10.1016/j.atmosenv.2009.09.002.

Pacifico, F., S. P. Harrison, C. D. Jones, A. Arneth, S. Sitch, G. P. Weedon, M. P. Barkley, P. I. Palmer, D. Serça, M. Potosnak, T.-M. Fu, A. Goldstein, J. Bai, and G. Schurgers (2011), Evaluation of a photosynthesis-based biogenic isoprene emission scheme in JULES and simulation of isoprene emissions under present-day climate conditions, *Atmospheric Chemistry and Physics*, *11*(9), 4371–4389, doi:10.5194/acp-11-4371-2011.

Pacifico, F., G. A. Folberth, S. Sitch, J. M. Haywood, L. V. Rizzo, F. F. Malavelle, and P. Artaxo (2015), Biomass burning related ozone damage on vegetation over the amazon forest: a model sensitivity study, *Atmospheric Chemistry and Physics*, *15*(5), 2791–2804, doi:10.5194/acp-15-2791-2015.

Pacifico, F., G. A. Folberth, C. D. Jones, S. P. Harrison, and W. J. Collins (2012), Sensitivity of biogenic isoprene emissions to past, present, and future environmental conditions and implications for atmospheric chemistry, *Journal of Geophysical Research-Atmospheres*, *117*, doi:10.1029/2012JD018276.

Parrella, J. P., D. J. Jacob, Q. Liang, Y. Zhang, L. J. Mickley, B. Miller, M. J. Evans, X. Yang, J. A. Pyle, N. Theys, and M. Van Roozendael (2012), Tropospheric bromine chemistry: implications for present and pre-industrial ozone and mercury, *Atmospheric Chemistry And Physics*, *12*(15), 6723–6740, doi:10.5194/acp-12-6723-2012.

Pegoraro, E., A. Rey, E. G. Bobich, G. Barron-Gafford, K. A. Grieve, Y. Malhi, and R. Murthy (2004), Effect of elevated co_2 concentration and vapour pressure deficit on isoprene emission from leaves of *Populus deltoides* during drought, *Functional Plant Biology*, *31*(12), 1137–1147, doi:10.1071/FP04142.

Poschl, U., R. Von Kuhlmann, N. Poisson, and P. Crutzen (2000), Development and intercomparison of condensed isoprene oxidation mechanisms for global atmospheric

modelling, *Journal of Atmospheric Chemistry*, *37*, 29–52, doi:10.1023/A:1006391009798.

Possell, M., C. N. Hewitt, and D. J. Beerling (2005), The effects of glacial atmospheric co_2 concentrations and climate on isoprene emissions by vascular plants, *Global Change Biology*, *11*(1), 60–69.

Price, C., and D. Rind (1993), What determines the cloud -to-ground lightning fraction in thunderstorms?, *Geophysical Research Letters*, *20*(6), 463–466, doi:10.1029/93GL00226.

Ramankutty, N., and J. Foley (1999), Estimating historical changes in land cover: North American croplands from 1850 to 1992, *Global Ecology and Biogeography*, *8*, 381–396, doi:10.1046/j.1365-2699.1999.00141.x.

Rap, A., N. A. D. Richards, P. M. Forster, S. A. Monks, S. R. Arnold, and M. P. Chipperfield (2015), Satellite constraint on the tropospheric ozone radiative effect, *Geophysical Research Letters*, *42*(12), 5074–5081, doi:10.1002/2015GL064037.

Richards, J. (1990), Land transformation, in *The Earth as transformed by human action*, edited by B. Turner, R. Clark, W.C. Kates, J. Richards, J. Matthews, and W. Meyer, pp. 163–178, Cambridge University Press, Cambridge, United Kingdom and New York, NY, USA.

Riese, M., F. Ploeger, A. Rap, B. Vogel, P. Konopka, M. Dameris, and P. Forster (2012), Impact of uncertainties in atmospheric mixing on simulated utls composition and related radiative effects, *Journal of Geophysical Research: Atmospheres*, *117*(D16), n/a–n/a, doi:10.1029/2012JD017751, d16305.

Rossow, W. B., and R. A. Schiffer (1999), Advances in understanding clouds from ISCCP, *Bulletin Of The American Meteorological Society*, *80*(11), 2261–2287, doi:10.1175/1520-0477(1999)080¡2261:AIUCFI¿2.0.CO;2.

Ryerson, T., M. Trainer, J. Holloway, D. Parrish, L. Huey, D. Sueper, G. Frost, S. Donnelly, S. Schauffler, E. Atlas, W. Kuster, P. Goldan, G. Hubler, J. Meagher, and F. Fehsenfeld (2001), Observations of ozone formation in power plant plumes and implications for ozone control strategies, *SCIENCE*, *292*(5517), 719–723, doi: 10.1126/science.1058113.

Sanderson, M., W. Collins, C. Johnson, and R. Derwent (2006), Present and future acid deposition to ecosystems: The effect of climate change, *Atmospheric Environment*, *40*, 1275–1283, doi:http://dx.doi.org/10.1016/j.atmosenv.2005.10.031.

Shindell, D. T., G. Faluvegi, and N. Bell (2003), Preindustrial-to-present-day radiative forcing by tropospheric ozone from improved simulations with the giss chemistry-climate gcm, *Atmospheric Chemistry and Physics*, *3*(5), 1675–1702, doi:10.5194/acp-3-1675-2003.

Sillman, S. (2000), Ozone production efficiency and loss of NOx in power plant plumes: Photochemical model and interpretation of measurements in Tennessee, *Journal of Geophysical Research-Atmospheres*, *105*(D7), 9189–9202, doi:10.1029/1999JD901014.

Singh, H. B. (1987), Reactive nitrogen in the troposphere, *Environmental Science & Technology*, *21*(4), 320–327, doi:10.1021/es00158a001.

Sitch, S., P. M. Cox, W. J. Collins, and C. Huntingford (2007), Indirect radiative forcing of climate change through ozone effects on the land-carbon sink, *Nature*, *448*(7155), 791–U4, doi:10.1038/nature06059.

Skeie, R. B., T. K. Berntsen, G. Myhre, K. Tanaka, M. M. Kvalevåg, and C. R. Hoyle (2011), Anthropogenic radiative forcing time series from pre-industrial times until 2010, *Atmospheric Chemistry and Physics*, *11*(22), 11,827–11,857, doi:10.5194/acp-11-11827-

2011.

Smith, R., D. Fowler, M. Sutton, C. Flechard, and F. Coyle (2000), Regional estimation of pollutant gas dry deposition in the UK: model description, sensitivity analysis and outputs, *Atmospheric Environment*, *34*(22), 3757–3777, doi: http://dx.doi.org/10.1016/S1352-2310(99)00517-8.

Stevenson, D. S., P. J. Young, V. Naik, J.-F. Lamarque, D. T. Shindell, A. Voulgarakis, R. B. Skeie, S. B. Dalsoren, G. Myhre, T. K. Berntsen, G. A. Folberth, S. T. Rumbold, W. J. Collins, I. A. MacKenzie, R. M. Doherty, G. Zeng, T. P. C. van Noije, A. Strunk, D. Bergmann, P. Cameron-Smith, D. A. Plummer, S. A. Strode, L. Horowitz, Y. H. Lee, S. Szopa, K. Sudo, T. Nagashima, B. Josse, I. Cionni, M. Righi, V. Eyring, A. Conley, K. W. Bowman, O. Wild, and A. Archibald (2013), Tropospheric ozone changes, radiative forcing and attribution to emissions in the atmospheric chemistry and climate model intercomparison project (accmip), *Atmospheric Chemistry and Physics*, *13*(6), 3063–3085, doi:10.5194/acp-13-3063-2013.

Strada, S., and N. Unger (2016), Potential sensitivity of photosynthesis and isoprene emission to direct radiative effects of atmospheric aerosol pollution, *Atmospheric Chemistry and Physics*, *16*(7), 4213–4234, doi:10.5194/acp-16-4213-2016.

Tai, A. P. K., M. V. Martin, and C. L. Heald (2014), Threat to future global food security from climate change and ozone air pollution, *Nature Climate Change*, *4*(9), 817–821, doi:10.1038/NCLIMATE2317.

Turner, I., R. Moss, and D. Skole (1993), Relating land use and global land cover change. a proposal for an IGBP-HDP Core Project, IGBP Report no. 24, HDP Report no. 5. The International Geosphere-Biosphere Programme: A study of global change and the

Human Dimensions of Global Environmental Change Programme, Stockholm.

Unger, N. (2014), Human land-use-driven reduction of forest volatiles cools global climate, *Nature climate change*, *4*(10), 907–910, doi:10.1038/nclimate2347.

ValMartin, M., C. L. Heald, and S. R. Arnold (2014), Coupling dry deposition to vegetation phenology in the community earth system model: Implications for the simulation of surface o_3, *Geophysical Research Letters*, *41*(8), 2988–2996, doi:10.1002/2014GL059651.

Van Dingenen, R., F. J. Dentener, F. Raes, M. C. Krol, L. Emberson, and J. Cofala (2009), The global impact of ozone on agricultural crop yields under current and future air quality legislation, *Atmospheric Environment*, *43*(3), 604–618, doi: http://dx.doi.org/10.1016/j.atmosenv.2008.10.033.

Wang, Y., J. A. Logan, and D. J. Jacob (1998), Global simulation of tropospheric O_3-NO_x-hydrocarbon chemistry: 2. model evaluation and global ozone budget, *Journal of Geophysical Research: Atmospheres*, *103*(D9), 10,727–10,755, doi:10.1029/98JD00157.

Wang, Y. H., and D. J. Jacob (1998), Anthropogenic forcing on tropospheric ozone and OH since preindustrial times, *Journal Of Geophysical Research-Atmospheres*, *103*(D23), 31,123–31,135, doi:10.1029/1998JD100004.

Wesely, M. (1989), Parameterization of Surface Resistances to Gaseous Dry Deposition in Regional Scale Numerical Models, *Atmospheric Environment*, *23*(6), 1293–1304, doi: 10.1016/0004-6981(89)90153-4.

Wilkinson, M. J., R. K. Monson, N. Trahan, S. Lee, E. Brown, R. B. Jackson, H. W. Polley, P. A. Fay, and R. Fall (2009), Leaf isoprene emission rate as a function of atmospheric CO_2 concentration, *Global Change Biology*, *15*(5), 1189–1200, doi: 10.1111/j.1365-2486.2008.01803.x.

Worden, H. M., K. W. Bowman, S. S. Kulawik, and A. M. Aghedo (2011), Sensitivity of outgoing longwave radiative flux to the global vertical distribution of ozone characterized by instantaneous radiative kernels from aura-tes, *Journal of Geophysical Research: Atmospheres*, *116*(D14), n/a–n/a, doi:10.1029/2010JD015101, d14115.

Wu, S., L. J. Mickley, J. O. Kaplan, and D. J. Jacob (2012), Impacts of changes in land use and land cover on atmospheric chemistry and air quality over the 21st century, *Atmospheric Chemistry and Physics*, *12*(3), 1597–1609, doi:10.5194/acp-12-1597-2012.

Young, P. J., A. Arneth, G. Schurgers, G. Zeng, and J. A. Pyle (2009), The CO_2 inhibition of terrestrial isoprene emission significantly affects future ozone projections, *Atmospheric Chemistry and Physics*, *9*(8), 2793–2803, doi:10.5194/acp-9-2793-2009.

Young, P. J., A. T. Archibald, K. W. Bowman, J.-F. Lamarque, V. Naik, D. S. Stevenson, S. Tilmes, A. Voulgarakis, O. Wild, D. Bergmann, P. Cameron-Smith, I. Cionni, W. J. Collins, S. B. Dalsøren, R. M. Doherty, V. Eyring, G. Faluvegi, L. W. Horowitz, B. Josse, Y. H. Lee, I. A. MacKenzie, T. Nagashima, D. A. Plummer, M. Righi, S. T. Rumbold, R. B. Skeie, D. T. Shindell, S. A. Strode, K. Sudo, S. Szopa, and G. Zeng (2013), Pre-industrial to end 21st century projections of tropospheric ozone from the atmospheric chemistry and climate model intercomparison project (ACCMIP), *Atmospheric Chemistry and Physics*, *13*(4), 2063–2090, doi:10.5194/acp-13-2063-2013.

Yue, X., and N. Unger (2014), Ozone vegetation damage effects on gross primary productivity in the united states, *Atmospheric Chemistry and Physics*, *14*(17), 9137–9153, doi:10.5194/acp-14-9137-2014.

Table 1. Summary of HadGEM2-ES mid-19th century model scenarios to assess sensitivity of mid-19th century ozone to 1865 to 2000 land cover change.

Model Scenario	Land cover (LC)	Atmospheric CO_2	SST + Sea-ice	Chemistry and aerosol Emissions[a]
PI_CTRL	1865	286 ppmv (All of model)	1860s	1860s
VEG_2000	2000	286 ppmv (All of model)	1860s	1860s
CO2_DD	1865	368 ppmv (dry dep only)	1860s	1860s
CO2_DDBVOC	1865	368 ppmv (iBVOC + dry dep only)	1860s	1860s
CLIM_2000	2000	368 ppmv (All of model)	2000s	1860s
PD_2000	2000	368 ppmv (All of model)	2000s	2000s

[a] Surface emitted species include: NO_x, CH_4, CO, HCHO, C_2H_6, C_3H_8, Me_2CO, MeCHO, H_2, APIN, NVOC, MEK, C_4H_{10}, AROM, C_2H_4, C_3H_6.

Table 2. Global and regional differences in HadGEM2-ES PFT coverage in Mha between 1865 and 2000.

PFT	Globe	Tropics	NH mid-lats	SH mid-lats
Broadleaf Tree	-1092.4 Mha	-721.9 Mha	-230.2 Mha	-140.9 Mha
Needleaf Tree	-218.5 Mha	-46.4 Mha	-150.7 Mha	-24.0 Mha
C3 Grass	1736.9 Mha	636.9 Mha	847.3 Mha	257.7 Mha
C4 Grass	933.0 Mha	548.4 Mha	228.5 Mha	156.8 Mha
Shrubs	-1404.1 Mha	-428.3 Mha	-726.1 Mha	-252.2 Mha

Table 3. Simulated changes in tropospheric ozone burden between each model scenario and the PI_CTRL scenario. All values are global annual averages. For reference the total column ozone for the PI_CTRL and PD_2000 simulations are 26.9DU and 35.0DU respectively.

Model Scenario[a]	Ozone Burden Tg O_3	ΔBurden Tg O_3	ΔTotal Column ozone DU
PI_CTRL	203.7 ± 9.4	-	-
VEG_2000	200.4 ± 8.8	-3.3	-0.2
CLIM_2000	205.0 ± 9.3	1.3	0.2
CO2_DD	204.5 ± 10.6	0.8	0.1
CO2_DDBVOC	204.1 ± 10.9	0.4	0.0
PD_2000	292.9 ± 18.4	89.2	8.1

[a] For reference the values from ACCMIP are 337 ± 23 Tg O_3, 98 ± 17 Tg O_3 and 8.4 ± 1.3 DU for ozone burden, ΔBurden and ΔTotal column ozone respectively [*Young et al.*, 2013; *Stevenson et al.*, 2013]. The ± values for our results are ± standard deviation on the annual burden value.

Table 4. Simulated changes in tropospheric ozone radiative effect (RE) between each mid-19th century scenario and the PI_CTRL scenario.

Model Scenario	ΔRE[a] W m^{-2}
VEG_2000	-0.012
CLIM_2000	0.001
CO2_DD	0.001
CO2_DDBVOC	0.001

[a] For reference the mid-19th century to present day radiative forcing (PI_CTRL to PD_2000) is 0.264 W m^{-2}.

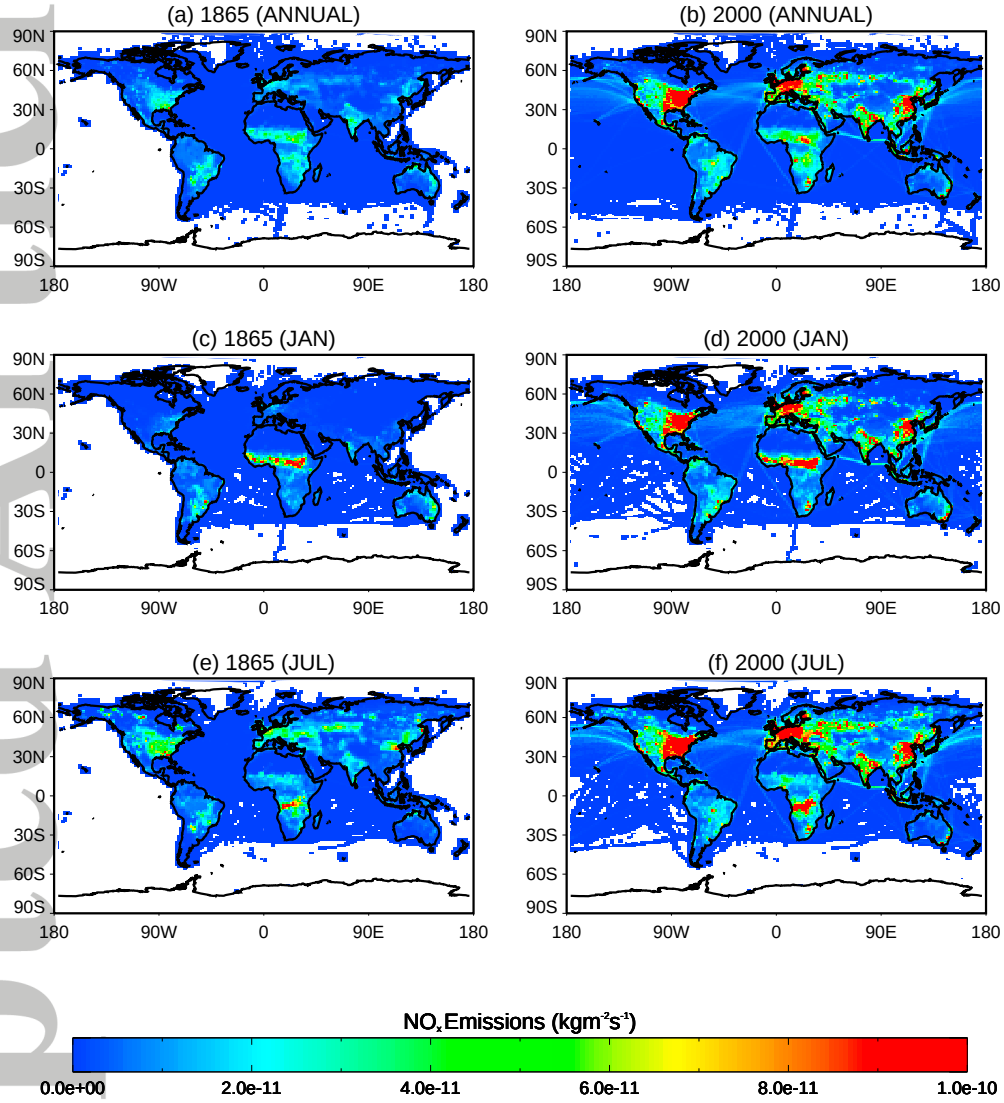

Figure 1. Global mean annual NO_x emissions for the 1860s under the PI_CTRL scenario (top panel). Monthly mean NO_x emissions are shown for January (middle panel) and July (bottom panel) to highlight the seasonality in emissions.

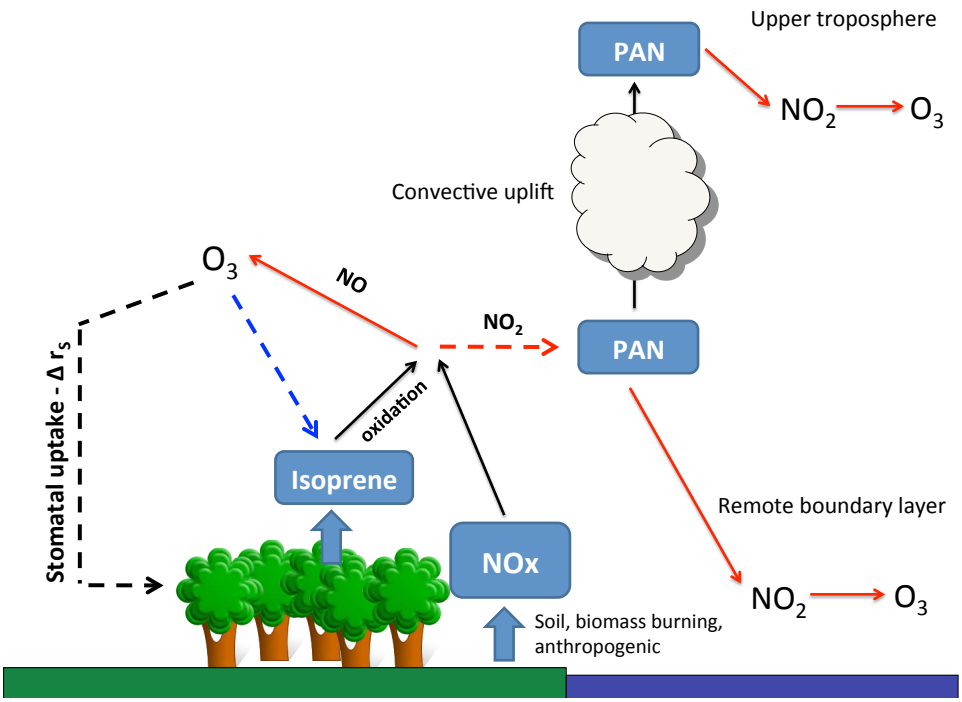

Figure 2. Chemical processes resulting from vegetation land cover change that impact tropospheric ozone. Blue arrows indicate processes dominant in low NO_x conditions, while red arrows are dominant in the presence of elevated NO_x. Dashed arrows show reactions or conversions that suppress ozone formation, while solid arrows enhance ozone formation. The formation of PAN from the reaction of NO_2 with isoprene oxidation products is a key pathway between changes in surface vegetation and ozone production and loss locally, over the remote marine regions and in the upper troposphere, where PAN can be transported in deep convection and frontal uplift.

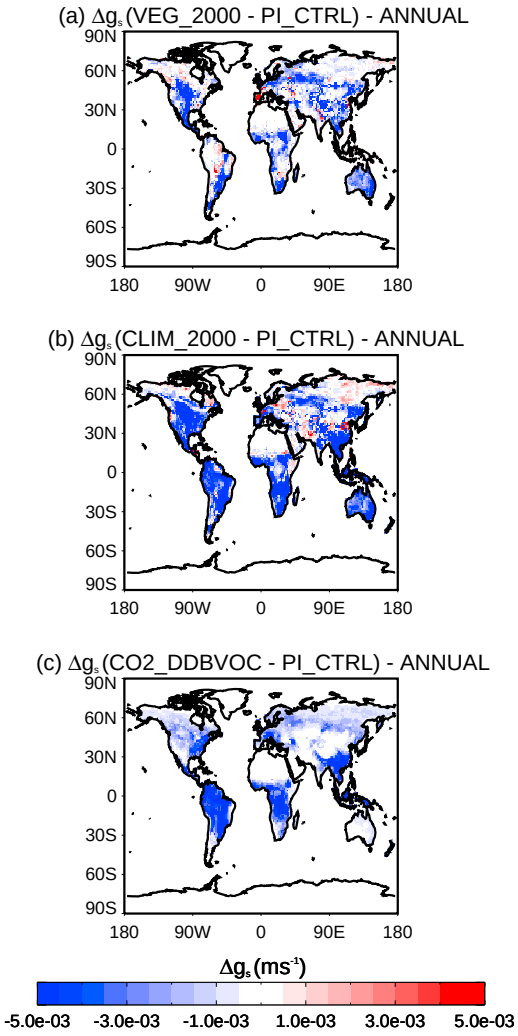

Figure 3. Changes in annual mean stomatal conductance (ms^{-1}) under the VEG_2000, 1860_EMS, CO2_DD and CO2_DDBVOC scenarios with respect to the PI_CTRL simulation. Note stomatal conductances are total gridbox stomatal conductance over all PFT types.

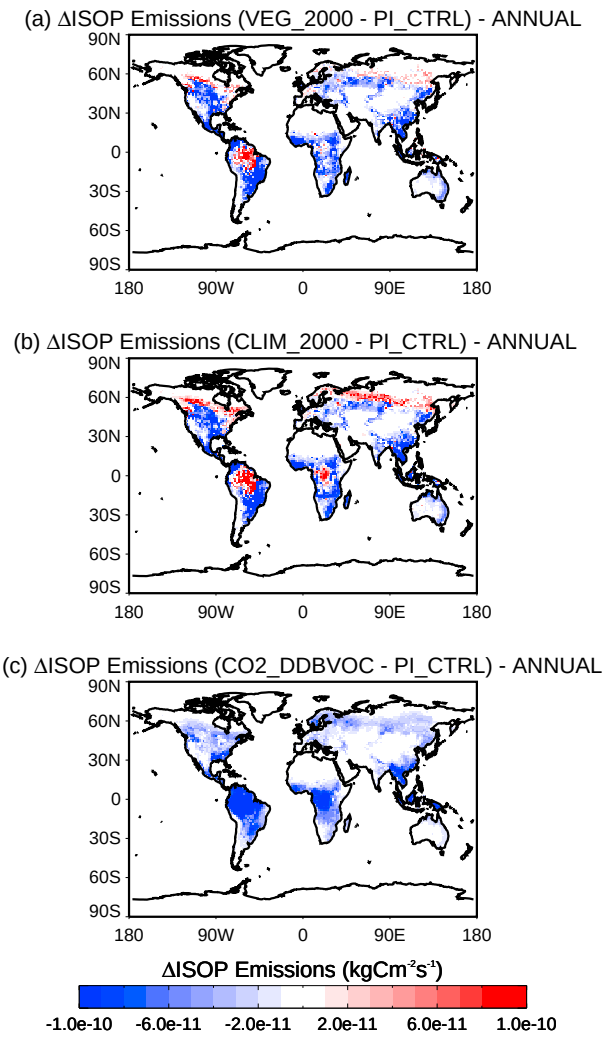

Figure 4. Changes in annual mean isoprene emissions ($kgCm^{-2}s^{-1}$) under the VEG_2000, 1860_EMS and CO2_DDBVOC scenarios with respect to the PI_CTRL simulation.

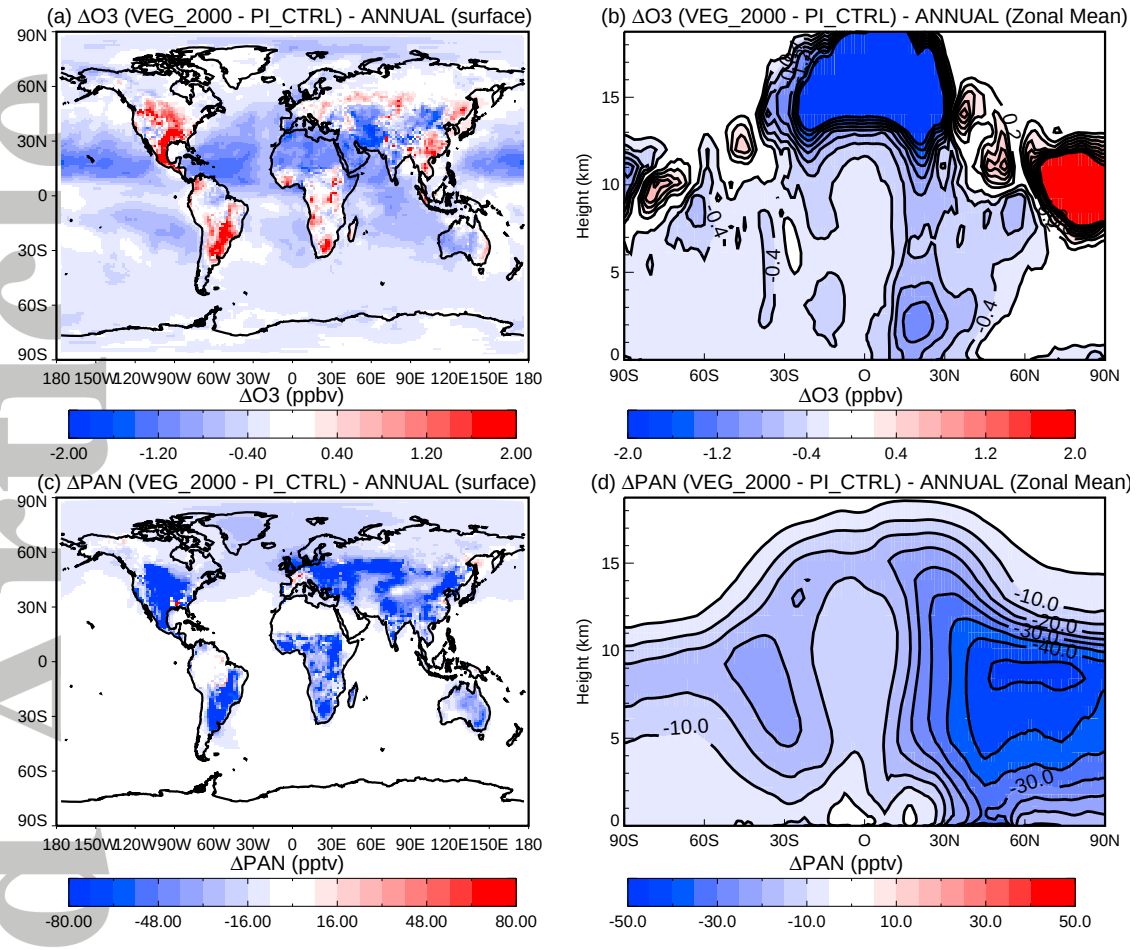

Figure 5. Changes in annual mean surface ozone (top left), annual mean zonal mean ozone (top right), annual mean surface PAN (bottom left) and annual mean zonal mean PAN (bottom right) under the VEG_2000 scenario with respect to the PI_CTRL simulation.

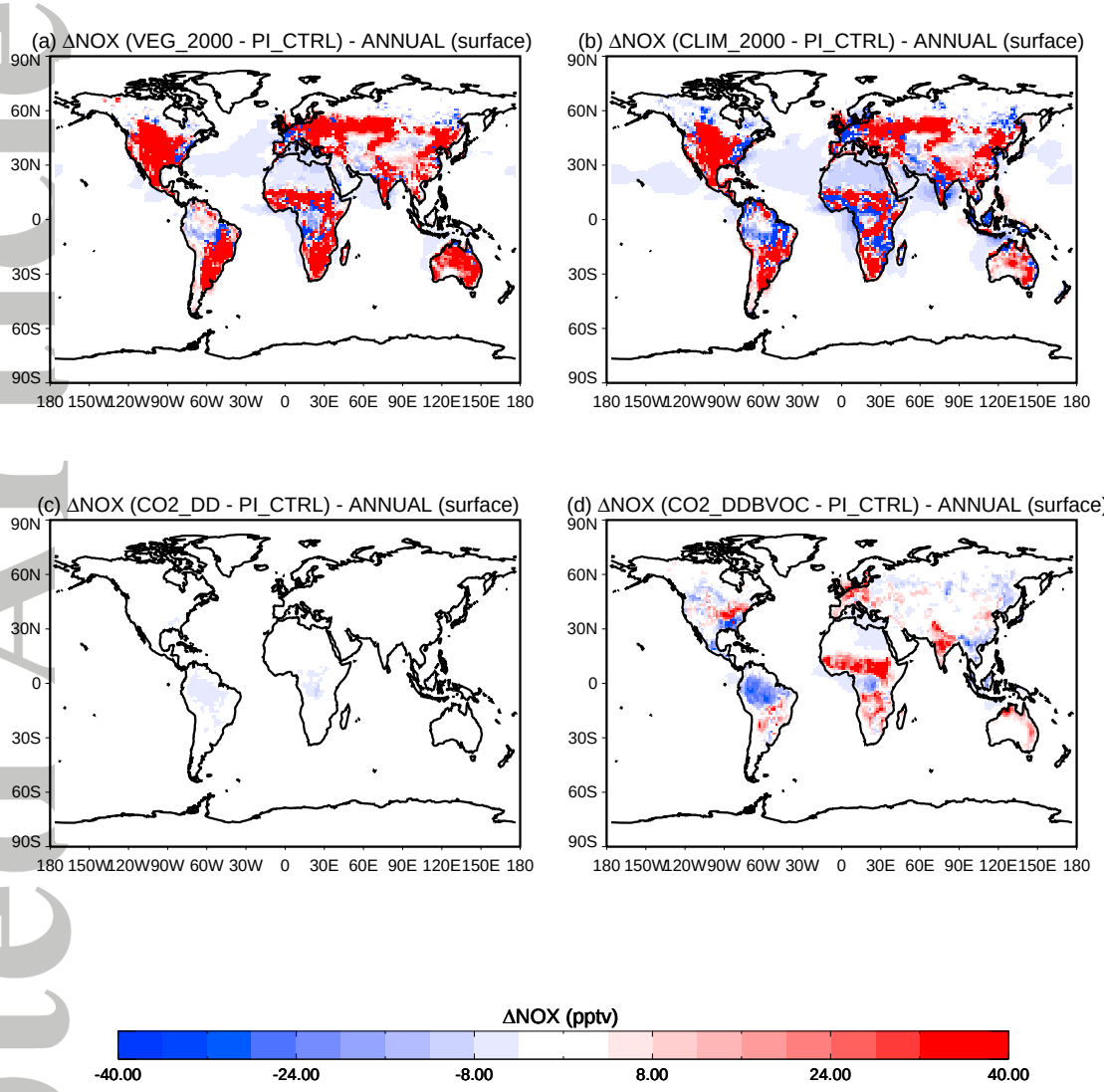

Figure 6. Changes in annual mean surface NO_x (pptv) under the VEG_2000, 1860_EMS, CO2_DD and CO2_DDBVOC scenarios with respect to the PI_CTRL simulation.

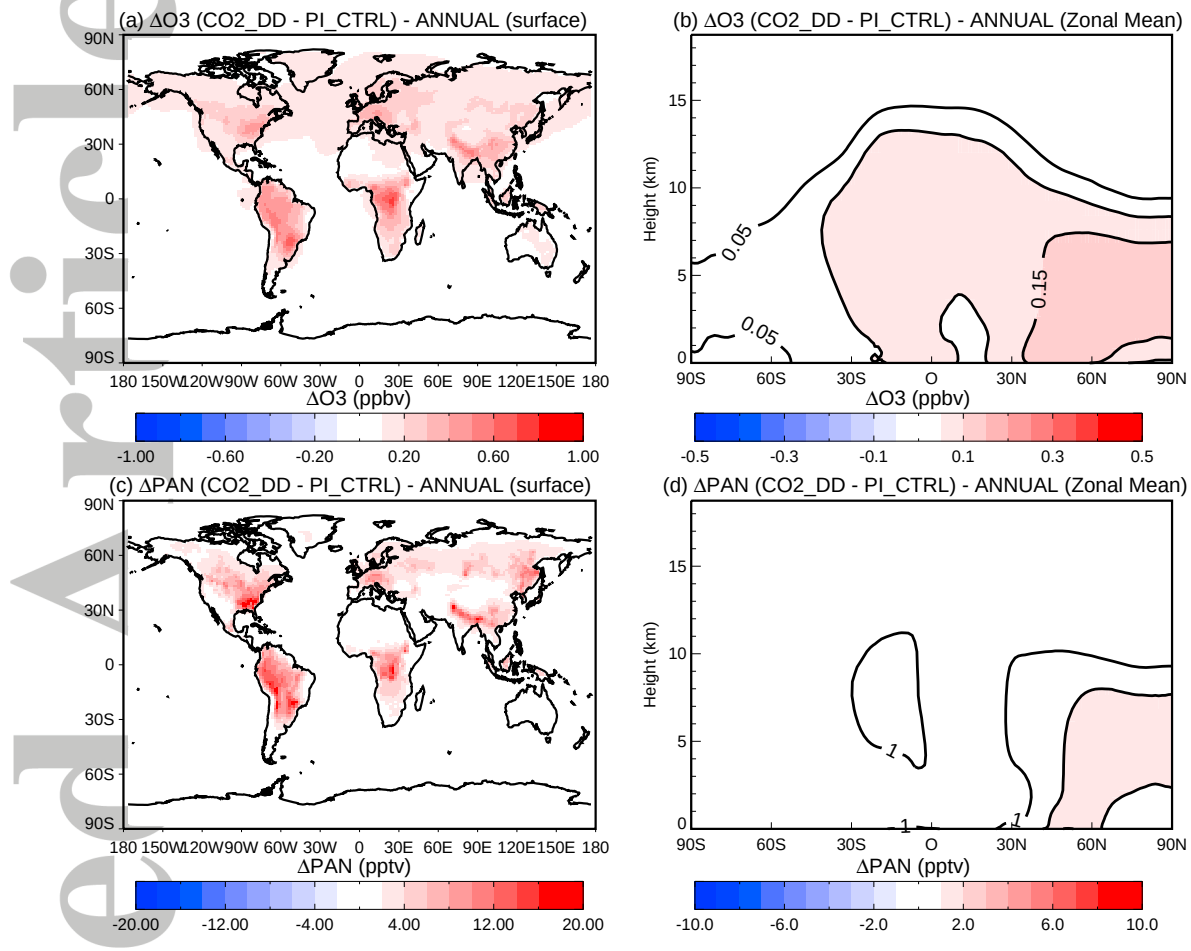

Figure 7. As Figure 5 except for the CO2_DD versus PI_CTRL scenarios

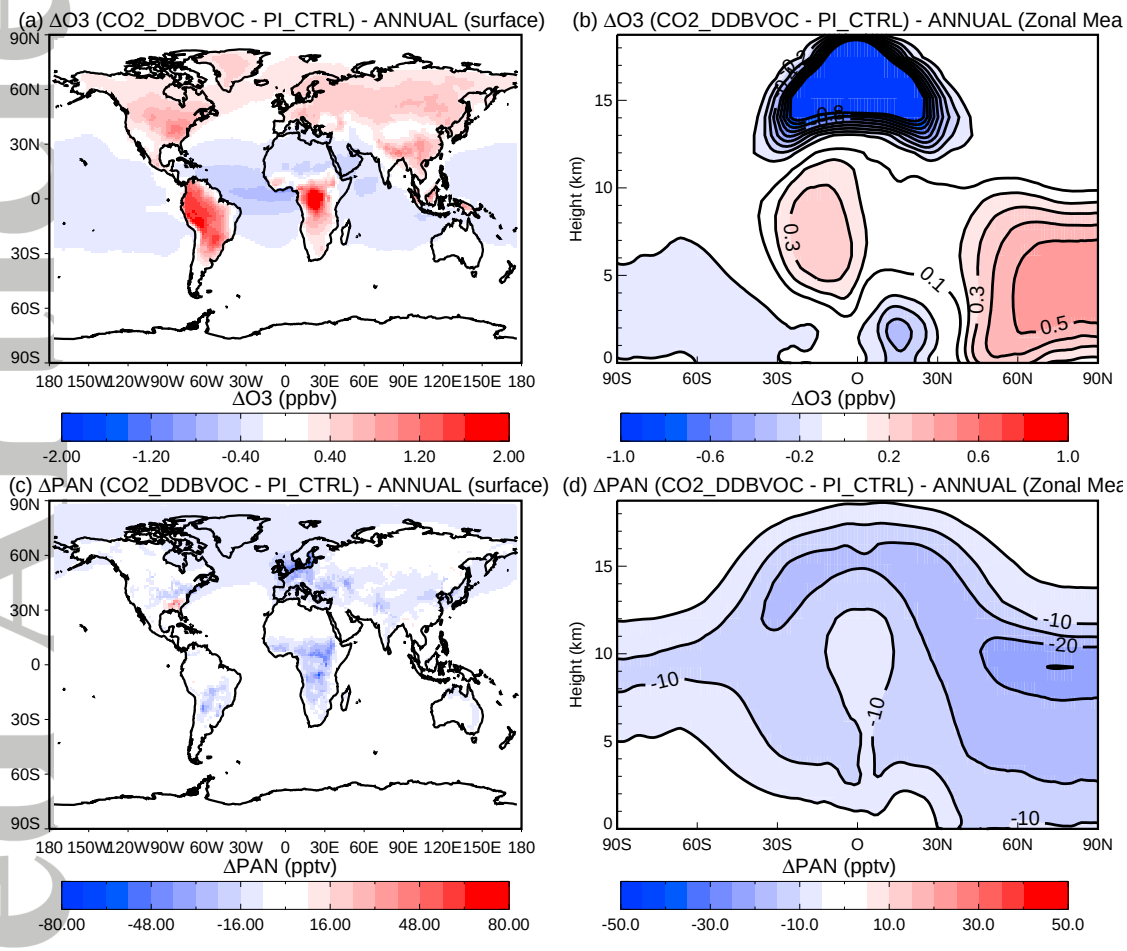

Figure 8. As Figure 5 except for the CO2_DDBVOC versus PI_CTRL scenarios

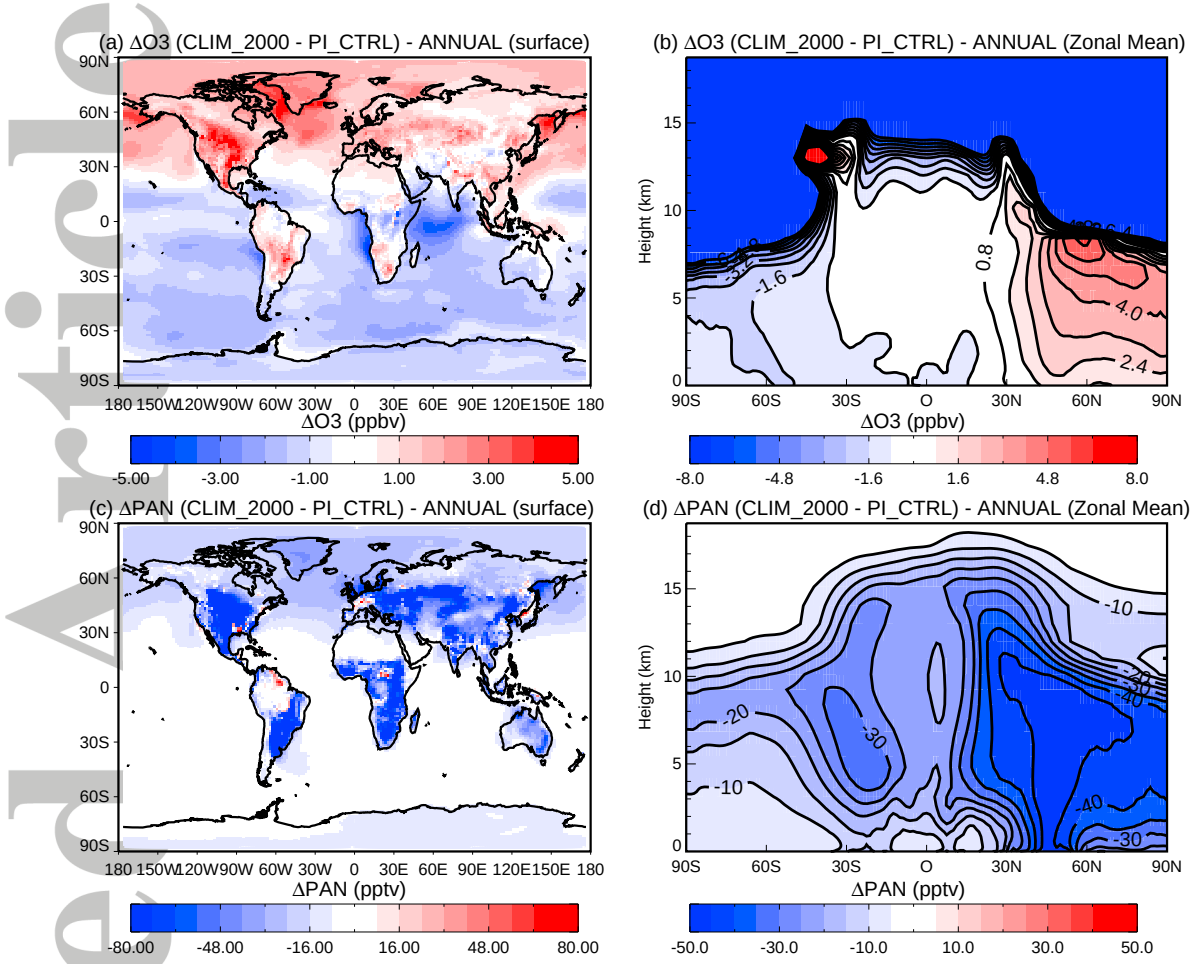

Figure 9. As Figure 5 except for the CLIM_2000 versus PI_CTRL scenarios. Note different scale on ozone changes.

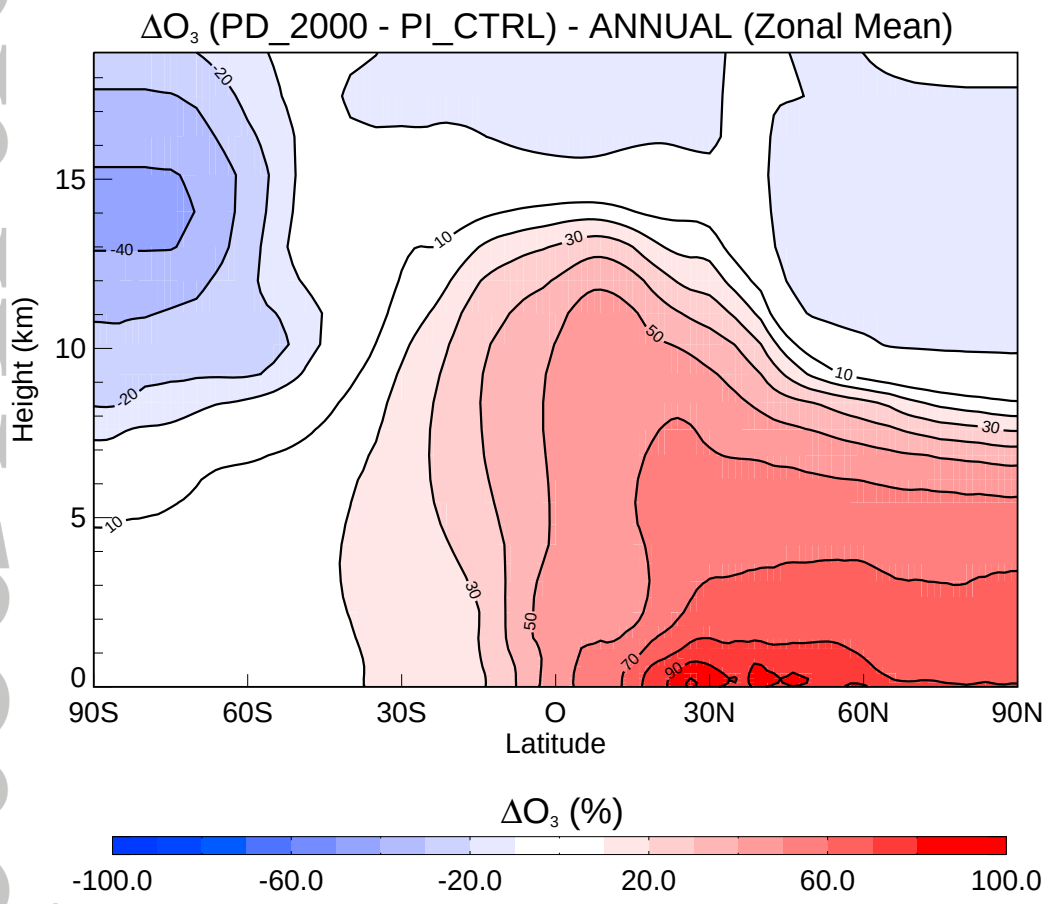

Figure 10. Percentage change of zonally averaged annual mean ozone from each of the mid-19th century ozone simulations to the present day.